

# Development of Serine Protease Inhibitors Displaying a Multicentered Short (<2.3 Å) Hydrogen Bond Binding Mode: Inhibitors of Urokinase-Type Plasminogen Activator and Factor Xa

Erik Verner,<sup>†</sup> Bradley A. Katz,<sup>‡</sup> Jeffrey R. Spencer,<sup>†</sup> Darin Allen,<sup>†</sup> Jason Hataye,<sup>†</sup> Witold Hruzewicz,<sup>†</sup> Hon C. Hui,<sup>†</sup> Aleksandr Kolesnikov,<sup>†</sup> Yong Li,<sup>†</sup> Christine Luong,<sup>‡</sup> Arnold Martelli,<sup>†</sup> Kesavan Radika,<sup>§</sup> Roopa Rai,<sup>†</sup> Miles She,<sup>†</sup> William Shrader,<sup>†</sup> Paul A. Sprengeler,<sup>‡</sup> Sean Trapp,<sup>†</sup> Jing Wang,<sup>§</sup> Wendy B. Young,<sup>†</sup> and Richard L. Mackman<sup>\*,†</sup>

Departments of Medicinal Chemistry, Structural Biology, and Biochemistry and Enzymology, Axys Pharmaceuticals Inc., 180 Kimball Way, South San Francisco, California 94080

Received February 8, 2001

Novel scaffolds that bind to serine proteases through a unique network of short hydrogen bonds to the catalytic Ser195 have been developed. The resulting potent serine protease inhibitors were designed from lead molecule 2-(2-hydroxyphenyl)-1*H*-benzimidazole-5-carboxamidinium, **6b**, which is known to display several modes of binding. For instance, **6b** can recruit zinc and bind in a manner similar to that reported by bis(5-amidino-2-benzimidazolyl)methane (BABIM) (*Nature* **1998**, 391, 608–612).<sup>1</sup> Alternatively, **6b** can bind in the absence of zinc through a multicentered network of short (<2.3 Å) hydrogen bonds. The lead structure was optimized in the zinc-independent binding mode toward a panel of six human serine proteases to yield optimized inhibitors such as 2-(3-bromo-2-hydroxy-5-methylphenyl)-1*H*-indole-5-carboxamidinium, **22a**, and 2-(2-hydroxybiphenyl-3-yl)-1*H*-indole-5-carboxamidinium, **22f**. Structure–activity relationships determined that, apart from the amidine function, an indole or benzimidazole and an *ortho* substituted phenol group were also essential components for optimal potency. The affinities (*K<sub>i</sub>*) of **22a** and **22f**, for example, bearing these groups ranged from 8 to 600 nM toward a panel of six human serine proteases. High-resolution crystal structures revealed that the binding mode of these molecules in several of the enzymes was identical to that of **6b** and involved short (<2.3 Å) hydrogen bonds among the inhibitor hydroxyl oxygen, Ser195, and a water molecule trapped in the oxyanion hole. In summation, novel and potent trypsin-like serine protease inhibitors possessing a unique mode of binding have been discovered.

## Introduction

Trypsin-like serine proteases are a family of proteolytic enzymes that have been implicated in many important biological processes, including blood coagulation, digestion, inflammation, metastasis, and cellular invasion.<sup>2</sup> Regulation of their biological action through small molecule inhibitors is therefore a potentially attractive way of treating many disease states. Perhaps the most actively researched member of the family with respect to the design of small molecule inhibitors is thrombin.<sup>3</sup> Other enzymes in the family, such as factor Xa, factor VIIa, tryptase, and, more recently, urokinase-type plasminogen activator (u-PA), are also receiving considerable attention.<sup>3–7</sup> Despite extensive efforts spanning several decades, there are few small molecule inhibitors of trypsin-like serine proteases widely available as drugs. One reason for the dearth of serine protease-targeted drugs is the criteria required for a therapeutically useful small molecule inhibitor of these enzymes. Inhibitors need to be highly potent, selective

among the closely related enzymes, and also possess adequate pharmacodynamic properties for the target of interest.

An early approach toward the design of potent inhibitors for serine proteases has been to develop molecules containing electrophiles, e.g., activated ketones, esters, aldehydes, boronic acids or esters, that achieve potency through the formation (or likely formation) of covalent adducts with the Ser195 or His57 (chymotrypsin numbering system) residues of the catalytic triad.<sup>8</sup> Figure 1 outlines some examples, **1–4**, of inhibitors of u-PA and other serine proteases that have been noted in the literature.<sup>6,9–11</sup> The covalent interaction tends to produce highly potent inhibitors which, in some circumstances, leads to very low rates of dissociation and essentially irreversible inhibition.<sup>6</sup> Selectivity in this type of inhibitor becomes critical and is typically generated through the elaboration of the chemical groups that occupy the subsites (S4–S3') around the catalytic machinery. The mere presence of the requisite electrophilic moieties in such inhibitors is viewed as detrimental to the identification of a drug since the chances of obtaining selectivity, oral availability, and minimal toxicity are severely compromised, prompting the search for noncovalent reversible inhibitors.

There are relatively few reports describing inhibitors that specifically and rationally exploit noncovalent

\* Corresponding author: Richard Mackman, Axys Pharmaceuticals Inc., 180 Kimball Way, South San Francisco, CA 94080. Tel: (650) 829-1191. Fax: (650) 829-1019. E-mail: richard\_mackman@axyspharm.com.

<sup>†</sup> Department of Medicinal Chemistry.

<sup>‡</sup> Department of Structural Biology.

<sup>§</sup> Department of Biochemistry and Enzymology.

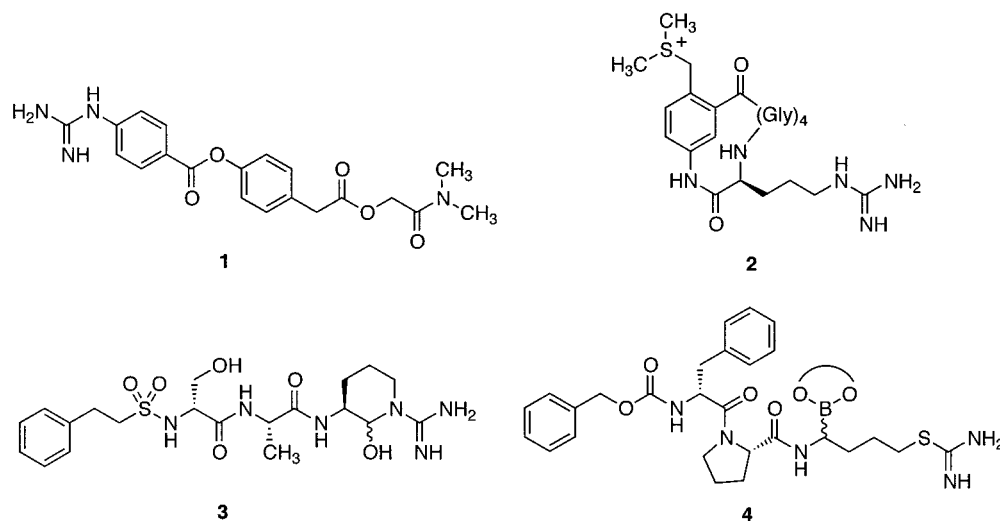


**Figure 1.** Inhibitors of u-PA and other proteases that contain electrophilic centers.

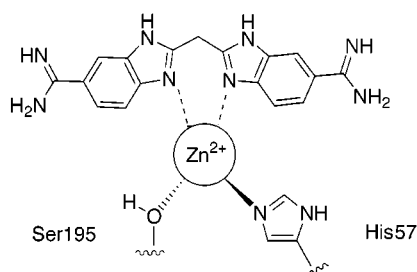


**Figure 2.** Schematic of BABIM binding to the catalytic Ser195 and His57 residues through recruitment of a zinc ion.

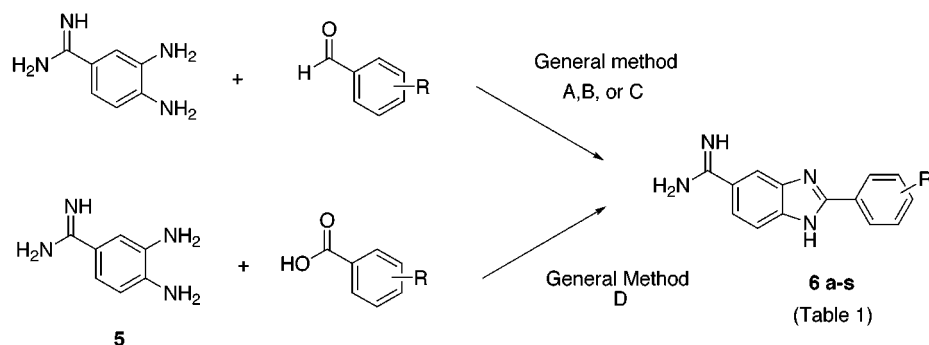
interactions with the common catalytic residues of serine proteases. Recently, a new and unusual high affinity binding mode for the serine protease inhibitor bis(5-amidino-2-benzimidazolyl)methane (BABIM) was identified whereby a zinc ion can be recruited to mediate binding between the inhibitor and the enzyme (Figure 2).<sup>1</sup> The zinc ion is tetrahedrally coordinated between two chelating nitrogen atoms of the inhibitor and the active site residues, Ser195 and His57. Molecules designed from the BABIM scaffold have displayed up to 5 orders of magnitude greater affinity toward enzymes in the serine protease family when assayed in the presence of zinc ions compared to zinc-free conditions (EDTA added).<sup>12</sup> As a consequence, highly potent and selective zinc-dependent inhibitors for important targets such as factor Xa and tryptase have been developed.<sup>12</sup> A potential obstacle to this approach of enzyme inhibition for future drug molecules is the high dependence on zinc for tight binding. Insufficient free zinc ions in the local environment of the target or a slow rate of complex formation may not be compatible for some drug targets. Sulfate ions have also been shown to mediate binding between a small molecule inhibitor and the catalytic machinery of trypsin.<sup>1,13</sup> The affinity enhancements in the sulfate-mediated binding mode are not as dramatic as those observed for the zinc-mediated binding mode.

We have sought to engineer inhibitors analogous to the zinc-mediated inhibitors that can bind to the catalytic residues through direct, rather than zinc-mediated, interactions. These inhibitors would potentially eliminate some of the kinetic and physiological concerns surrounding the zinc-mediated inhibitors and thus lead to a suite of compounds that nicely comple-

ments the zinc-mediated inhibitors. The molecule, 2-[2-hydroxyphenyl]-1*H*-benzimidazole-5-carboxamide, **6b** (Table 1), was found using high-resolution X-ray crystallography to display two distinct modes of binding in trypsin.<sup>14</sup> One mode is mediated through recruitment of a zinc ion similar to that described for BABIM, while the second mode involves the formation of a unique network of hydrogen bonds. The hydrogen bonds that are formed among Ser195, the inhibitor hydroxyl oxygen, and a water molecule trapped in the oxyanion hole are unusually short (2.0–2.3 Å) compared to ordinary hydrogen bonds (>2.6 Å). Exploration of structure–activity relationships (SAR) has resulted in optimization of the lead **6b** into several inhibitors, for example, **22a** and **22f**, that display affinities ( $K_i$ ) in the 8–600 nM range toward a panel of six common human serine proteases (Table 2). The binding of the optimized inhibitors was demonstrated to be through an identical multicentered network of short and normal range hydrogen bonds. To our knowledge, the unique multicentered short hydrogen-bonding network displayed by these inhibitors is unprecedented in the literature. Thus, a complementary class of potent serine protease inhibitors based on the scaffold **6b**, displaying a unique binding mode, has now evolved. The inhibitor **22f** is currently being exploited for the development of potent and specific inhibitors of u-PA whereas the alternative inhibitor, **22a**, has been optimized into a series of selective factor Xa inhibitors.<sup>15</sup> This report focuses on the synthesis and potency optimization of the lead scaffold **6b** that led to the identification of inhibitors **22a** and **22f** along with the structural characterization of the short hydrogen bond-mediated binding mode.

## Chemistry

A typical procedure for the formation of 5-amidino-benzimidazoles involves the condensation of 3,4-diaminobenzamide or 3,4-diaminobenzonitrile with either an imide<sup>16,17</sup> or an acid,<sup>17,18</sup> followed by conversion of the nitrile to an amidine using a modified Pinner reaction.<sup>16</sup> Two more recent reports<sup>19</sup> have utilized the condensation of 3,4-diaminobenzamide with a benzaldehyde followed by oxidation of the intermediate dihydrobenzimidazole to yield 5-amidinobenzimidazoles. A combination of some of these reported methods (general methods

Scheme 1<sup>a</sup>

<sup>a</sup> Reagents and conditions: General method A: EtOH, reflux, 10–50% yield. General method B: *N,N*-dimethylacetamide, Na<sub>2</sub>S<sub>2</sub>O<sub>5</sub>, 100 °C, 22% yield. General method C: 1,4-benzoquinone, EtOH, reflux, 89% yield. General method D: PPA, 180 °C, 10–30% yield.

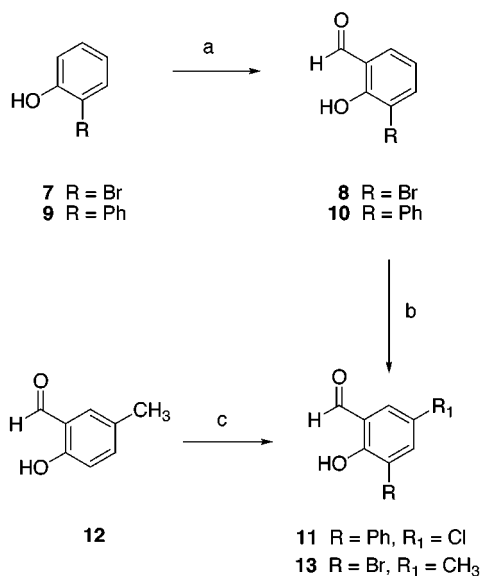
Table 1. Effect of Aryl Substitution on Enzyme Inhibition

no.	R					formula	procedure	<i>K<sub>i</sub></i> (μM)					
	2'	3'	4'	5'	6'			u-PA	t-PA	factor Xa	thrombin	plasmin	trypsin
<b>6a</b>	H	H	H	H	H	C <sub>14</sub> H <sub>12</sub> N <sub>4</sub>	A	55	381	125	340	350	55
<b>6b</b>	OH	H	H	H	H	C <sub>14</sub> H <sub>12</sub> N <sub>4</sub> O	A	5.5	75	14	55	46	23
<b>6c</b>	OH	H	H	NO <sub>2</sub>	H	C <sub>14</sub> H <sub>11</sub> N <sub>5</sub> O <sub>3</sub>	A	3.3	56	7.8	34	41	30
<b>6d</b>	OH	H	H	F	H	C <sub>14</sub> H <sub>11</sub> FN <sub>4</sub> O	D	2.8	46	6.8	33	21	10
<b>6e</b>	OH	H	H	Br	H	C <sub>14</sub> H <sub>11</sub> BrN <sub>4</sub> O	D	3.7	41	5.7	37	29	14
<b>6f</b>	OH	H	H	Me	H	C <sub>15</sub> H <sub>14</sub> N <sub>4</sub> O	A	7.5	113	16	65	60	9.0
<b>6g</b>	OH	H	H	OMe	H	C <sub>15</sub> H <sub>14</sub> N <sub>4</sub> O <sub>2</sub>	A	3.6	63	8.9	41	25	6.5
<b>6h</b>	OH	NO <sub>2</sub>	H	H	H	C <sub>14</sub> H <sub>11</sub> N <sub>5</sub> O <sub>3</sub>	D	0.90	14	1.3	1.1	15	8.5
<b>6i</b>	OH	F	H	H	H	C <sub>14</sub> H <sub>11</sub> FN <sub>4</sub> O	C	0.55	10	0.89	7.0	5.5	3.5
<b>6j</b>	OH	Br	H	H	H	C <sub>14</sub> H <sub>11</sub> BrN <sub>4</sub> O	B	0.25	3.4	0.30	2.3	1.7	1.4
<b>6k</b>	OH	Me	H	H	H	C <sub>15</sub> H <sub>14</sub> N <sub>4</sub> O	D	8.0	69	10	48	60	15
<b>6l</b>	OH	OMe	H	H	H	C <sub>15</sub> H <sub>14</sub> N <sub>4</sub> O <sub>2</sub>	A	3.6	69	16	80	19	30
<b>6m</b>	OH	Ph	H	H	H	C <sub>20</sub> H <sub>16</sub> N <sub>4</sub> O	D	0.40	1.0	2.1	15	5.0	6.5
<b>6n</b>	OH	H	Me	H	H	C <sub>15</sub> H <sub>14</sub> N <sub>4</sub> O	D	3.6	48	9.4	38	35	18
<b>6o</b>	OH	H	NEt <sub>2</sub>	H	H	C <sub>18</sub> H <sub>21</sub> N <sub>5</sub> O	A	13	100	25	90	80	16
<b>6p</b>	OH	H	H	H	OH	C <sub>14</sub> H <sub>12</sub> N <sub>4</sub> O <sub>2</sub>	D	1.9	25	5.0	17	7.5	6.0
<b>6q</b>	OH	-naphthyl-	H	H	H	C <sub>18</sub> H <sub>14</sub> N <sub>4</sub> O	A	3.9	31	9.9	80	33	18
<b>6r</b>	OH	Br	H	Me	H	C <sub>15</sub> H <sub>13</sub> BrN <sub>4</sub> O	A	0.28	2.4	0.57	2.7	3.2	3.3
<b>6s</b>	OH	Ph	H	Cl	H	C <sub>20</sub> H <sub>15</sub> ClN <sub>4</sub> O	A	0.50	0.28	0.94	12	4.1	3.3

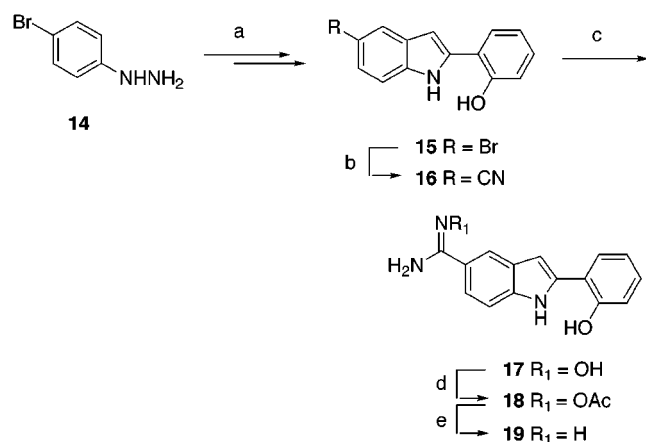
A–D in Scheme 1), incorporating some minor modifications, were used to synthesize the benzimidazole analogues **6a–s**. General methods A, B, and C involve the condensation of a substituted benzaldehyde with 3,4-diaminobenzamidine dihydrochloride **5**. In the presence of 1,4-benzoquinone, the desired benzimidazole was formed rapidly and in good yield, but removal of trace amounts of 1,4-benzoquinone and related products was problematic, often requiring laborious chromatography (general procedure C). Sodium metabisulfite was found to facilitate the oxidation step and was easier to remove compared to 1,4-benzoquinone (general procedure B). The absence of oxidizing agents in the reaction also gave the desired product, presumably through slow atmospheric oxidation (general procedure A). Most of the analogues shown in Table 1 were generated by procedure A, since it eliminated the need to remove an oxidizing agent in workup. In the examples where it was more convenient to use a commercially available benzoic acid, the procedure of Fairley et al. was used.<sup>17</sup> Thus, 3,4-diaminobenzamidine was condensed with the corresponding benzoic acid in polyphosphoric acid (PPA) at high temperature (general method D). The 3,4-

diaminobenzamidine reagent **5** which was used in general methods A–D was synthesized using literature procedures.<sup>17</sup> The products were purified by reverse phase HPLC, and the yields were typically in the 10–50% range. Most of the aryl aldehydes and acids were commercially available except for those obtained according to Scheme 2. 2-Bromophenol **7** was treated with paraformaldehyde in the presence of base and MgCl<sub>2</sub> to form benzaldehyde **8**.<sup>20</sup> The same procedure was also used to synthesize aldehyde **10** from biphenyl-2-ol **9**. Chlorination of **10** using the reagent *N*-chlorosuccinimide (NCS) gave benzaldehyde **11**. Compound **13** was prepared from commercially available benzaldehyde **12** using bromine in acetic acid.

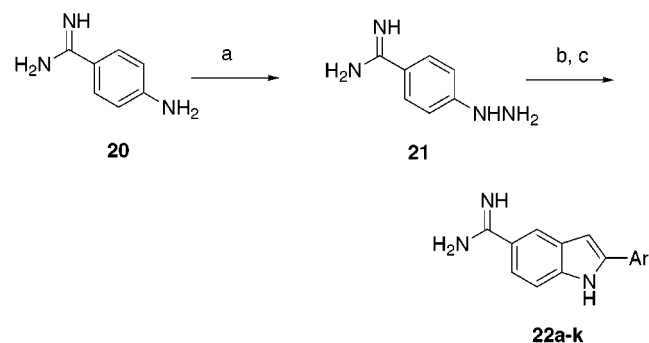
The synthesis of compounds containing a 5-amidinoindole group instead of a 5-amidinobenzimidazole was also based on existing literature procedures (Schemes 3 and 4).<sup>16,21</sup> Scheme 3 depicts the sequence of steps used to make 5-amidinoindole **19**, a compound previously reported by Iwanowicz and co-workers.<sup>21</sup> Nitrile **16** was prepared<sup>21</sup> and then converted to the 5-amidinoindole product **19**, through formation of the hydroxyamidine **17** and acetoxyamidine **18**. A shorter but

Scheme 2<sup>a</sup>

<sup>a</sup> Reagents and conditions: (a) MgCl<sub>2</sub>, Et<sub>3</sub>N, (CH<sub>2</sub>O)<sub>n</sub>, reflux; (b) NCS, AcOH, reflux; (c) bromine, AcOH.

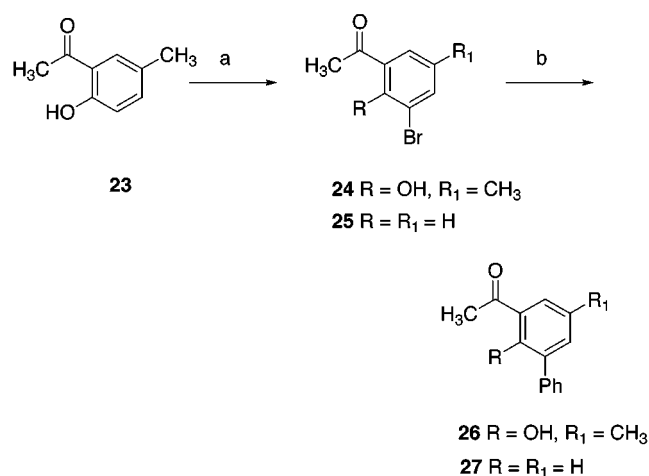
Scheme 3<sup>a</sup>

<sup>a</sup> Reagents and conditions: (a) Iwanowicz;<sup>21</sup> (b) CuCN, 220 °C, quinoline; (c) 50% NH<sub>2</sub>OH (aq), EtOH, reflux; (d) Ac<sub>2</sub>O, AcOH, THF; (e) H<sub>2</sub>, Pd/C 10%.

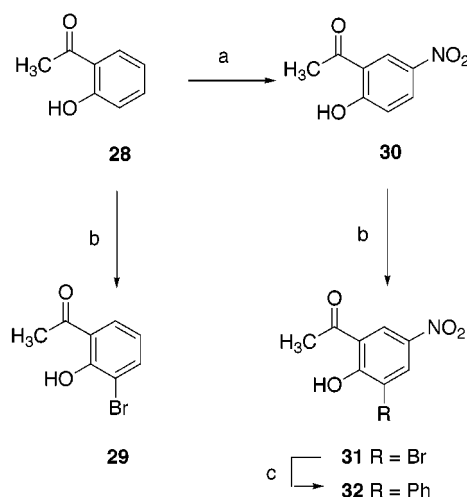
Scheme 4<sup>a</sup>

<sup>a</sup> Reagents and conditions: (a) NaNO<sub>2</sub>, 6 N HCl, 0 °C then SnCl<sub>2</sub>·2H<sub>2</sub>O; (b) ArCOCH<sub>3</sub>, EtOH, Et<sub>3</sub>N, reflux; (c) PPA, 140–160 °C, 5–71% yield.

lower yielding approach based on the Fischer Indolization was used for all the other examples **22a–k** in Table 2 (Scheme 4).<sup>16,22</sup> Hydrazine **21** was prepared from aniline **20** according to the hydrazine preparation conditions described by Castro et al. for the synthesis

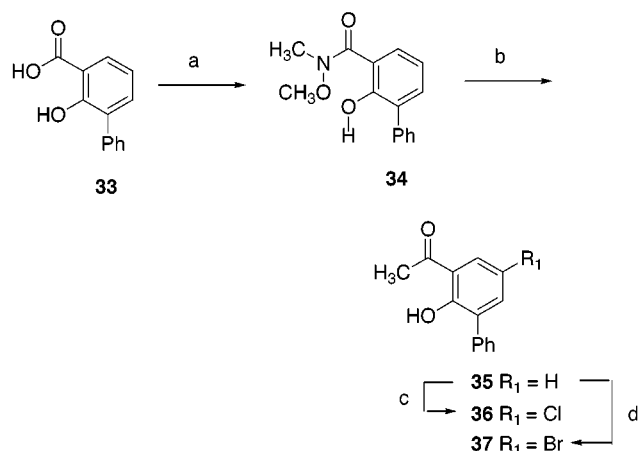
Scheme 5<sup>a</sup>

<sup>a</sup> Reagents and conditions: (a) MeOH, NBS; (b) C<sub>6</sub>H<sub>5</sub>B(OH)<sub>2</sub>, Pd(PPh<sub>3</sub>)<sub>4</sub>, base, H<sub>2</sub>O, 75 °C.

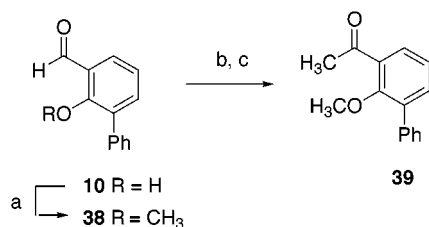
Scheme 6<sup>a</sup>

<sup>a</sup> Reagents and conditions: (a) fuming HNO<sub>3</sub>, AcOH, 0 °C; (b) NBS, AcOH; (c) C<sub>6</sub>H<sub>5</sub>B(OH)<sub>2</sub>, Pd(PPh<sub>3</sub>)<sub>4</sub>, 10% Na<sub>2</sub>CO<sub>3</sub>, THF, 80 °C.

of 4-hydrazinobenzonitrile.<sup>23</sup> Hydrazine **21** was then condensed with the desired acetophenones to give hydrazones. High temperature treatment of the hydrazones in PPA then resulted in cyclization to the indoles. Purification of the products from the PPA reagent required reverse phase preparative HPLC chromatography. A drawback of this method was the need to remove phosphorylated side products, leading to lower than expected yields, typically in the 10–30% range. The acetophenones required for analogues **22a–k** were either commercially available or conveniently synthesized using the methods shown in Schemes 5–8. Aryl bromide **24** was prepared in 85% yield by treatment of **23** with *N*-bromosuccinimide (NBS) (Scheme 5). The two aryl bromides **24** and commercially available **25** were then converted in high yield to biaryls **26** and **27**, respectively, using Suzuki conditions.<sup>24</sup> Nitration of **28** with fuming nitric acid yielded 1-(2-hydroxy-5-nitrophenyl)ethanone **30** (Scheme 6). Subsequent reaction of both **28** and **30** with NBS resulted in the formation of aryl bromides **29** and **31**, respectively. The *para* isomer of **29** was the main product in the reaction of **28** with NBS, but sufficient amounts of the desired *ortho* sub-

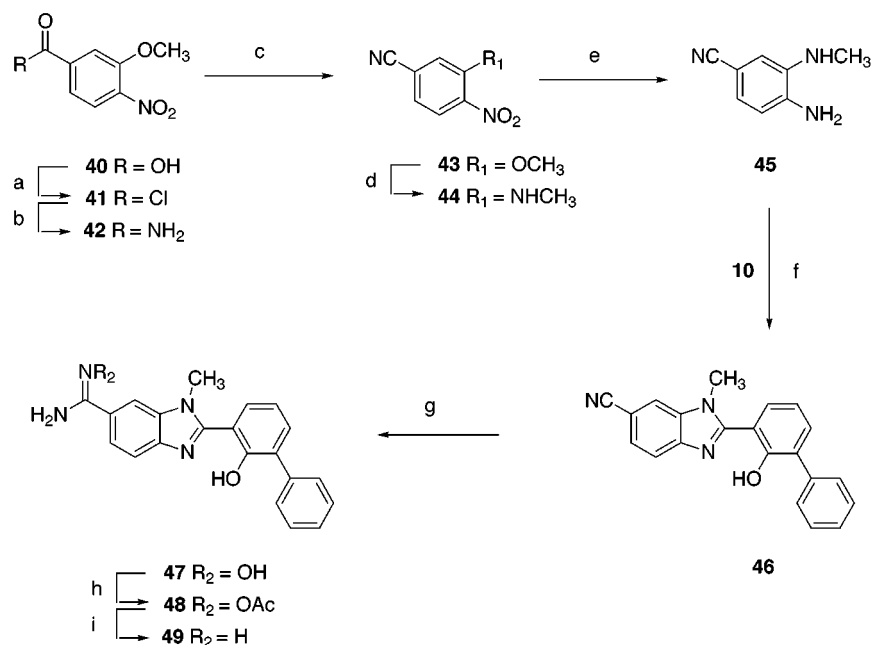
Scheme 7<sup>a</sup>

<sup>a</sup> Reagents and conditions: (a) *N,O*-dimethylhydroxylamine hydrochloride, PyBOP, DIEA, DMF, 0 °C; (b) MeLi, 0 °C, Et<sub>2</sub>O; (c) NCS, DMF; (d) NBS, AcOH, 85 °C.

Scheme 8<sup>a</sup>

<sup>a</sup> Reagents and conditions: (a) CH<sub>3</sub>I, Cs<sub>2</sub>CO<sub>3</sub>, DMF; (b) CH<sub>3</sub>MgBr, VCl<sub>3</sub>, CH<sub>2</sub>Cl<sub>2</sub>, -78 °C; (c) TPAP, 4-methylmorpholine-*N*-oxide, CH<sub>2</sub>Cl<sub>2</sub>.

stituted isomer could be isolated. Similar conditions to those used for the formation of biaryls **26** and **27** were then used to generate biaryl **32**. The sequence of steps used to synthesize acetophenones **35**–**37** from 3-phenylsalicylic acid **33** is shown in Scheme 7. The

Scheme 9<sup>a</sup>

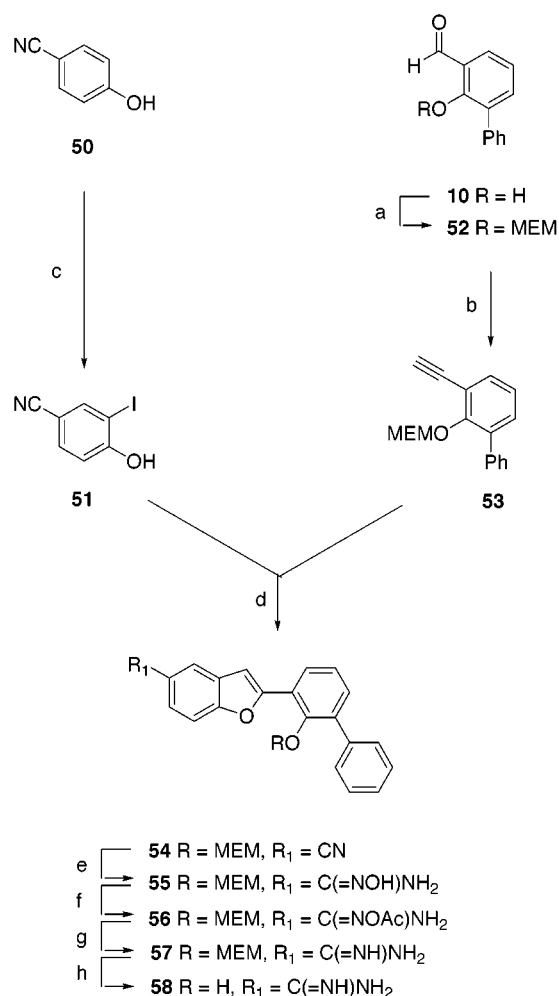
<sup>a</sup> Reagents and conditions: (a) (COCl)<sub>2</sub>, DMF, THF, 0 °C; (b) NH<sub>3</sub>, THF, 0 °C; (c) TFA, Et<sub>3</sub>N, THF; (d) 40% methylamine (aq.), DMSO, 75 °C; (e) H<sub>2</sub>, Pd/C 10%, MeOH, EtOAc; (f) 10, general procedure C; (g) 50% NH<sub>2</sub>OH (aq.), DMSO, 70 °C; (h) Ac<sub>2</sub>O, AcOH; (i) H<sub>2</sub>, Pd/C 10%, AcOH.

Weinreb amide **34** was formed from **33** and was then treated with methyllithium at 0 °C to generate acetophenone **35** in 47% yield over the two steps. The acetophenone **35** was then readily transformed to **36**, using NCS, and also to **37**, using NBS. Acetophenone **39** was prepared according to Scheme 8. Benzaldehyde **10** was treated with methyllithium in the presence of cesium carbonate to form 2-methoxybiphenyl-3-carbaldehyde **38** in 56% yield. The aldehyde **38** was then converted to **39** in 70% yield by treatment with vanadium(III) chloride and MeMgBr followed by oxidation of the intermediate alcohol using tetrapropylammonium perruthenate (TPAP) and 4-methylmorpholine-*N*-oxide.

To prepare alternative S1 binding heterocycles such as the methyl substituted benzimidazole **49**, the synthetic route in Scheme 9 was employed. Nitrile **43** was prepared from acid **40** in 69% overall yield through the formation of the acid chloride **41** and amide **42**. Displacement of the methoxy group by methylamine was readily performed in DMSO at 75 °C to give arylamine **44**. Reduction of **44** over Pd/C to diamine **45** was then followed by condensation with aldehyde **10** according to general scheme C (see above) to give the benzimidazole **46** (77% yield from **43**). The final conversion of benzimidazole **46** to 5-amidinobenzimidazole **49** proceeded in 33% yield, through the same sequence of steps used for the synthesis of **19** from **16**.

The synthesis of the benzofuran analogue, **58**, is outlined in Scheme 10 and is based on a palladium-mediated coupling of an alkyne with an aryl halide. Treatment of 4-hydroxybenzonitrile **50** with *N*-iodosuccinimide (NIS) gave aryl halide **51**. The hydroxyl group on benzaldehyde **10** was protected with 2-methoxyethoxymethyl (MEM) chloride. It was important to protect the hydroxyl group prior to formation of alkyne **53** in order to prevent intramolecular benzofuran formation. The protected aldehyde **52** was converted to



Scheme 10<sup>a</sup>

alkyne **53** using the (1-diazo-2-oxopropyl)phosphoric acid dimethyl ester reagent.<sup>25</sup> Coupling of alkyne **53** with aryl halide **51** under similar conditions to those described by Candiani<sup>26</sup> gave the benzofuran, **54**, in 23% yield. The benzofuran **54** was then converted to **57** using the sequence of steps described for the preparation of **19** from **16**. Final removal of the MEM protecting group with hydrochloric acid gave the desired product, **58**, in 43% yield from **54**.

**Biological Activity**

All the compounds were tested against a panel of six human trypsin-like serine proteases: u-PA, tissue-type plasminogen activator (t-PA), factor Xa, thrombin, plasmin, and trypsin. Ethylenediaminetetraacetic acid (EDTA) was used to remove zinc ions thereby eliminating any zinc-mediated binding effects in the assay that can occur for some of these scaffolds. The assay was buffered at pH = 7.4 in order to mimic physiological pH. Apparent inhibition constants were converted to *K<sub>i</sub>* values as described in the Experimental Section.<sup>27</sup>

### Biological Activity

**Results and Discussion**

The screening of libraries of compounds containing amidine-bearing heterocycles yielded compound **6b**

(Table 1) as a low micromolar inhibitor toward a panel of six human serine proteases. The scaffold has several notable attributes, including a low molecular weight (<300 amu), nonpeptidic character, and a convenient synthesis from diaminobenzamidine and a salicylic acid (or salicylaldehyde), making structure–activity relationships relatively straightforward to explore. The affinity measured at pH = 7.4 for the six enzymes, in the absence of free zinc ions, ranged from 5.5 to 75 μM (Table 1). The high-resolution X-ray structure of the zinc-independent binding mode of **6b** in trypsin and in u-PA (Figure 3) shows that binding of the inhibitor is mediated by a series of hydrogen bonds, three of which are very short (<2.3 Å) (Table 3). This unique multi-centered short hydrogen bond-mediated binding mode is shown schematically in Figure 4. Briefly, the short hydrogen bonds involve a triangle of oxygens comprising the inhibitor oxygen (O2'), a water co-bound in the oxyanion hole (H<sub>2</sub>O<sub>oxy</sub>) and the catalytic serine (Oγ<sub>Ser195</sub>). The distances in the u-PA complex of **6b** are O2'–Oγ<sub>Ser195</sub> = 2.14 Å, H<sub>2</sub>O<sub>oxy</sub>–Oγ<sub>Ser195</sub> = 2.30 Å, and H<sub>2</sub>O<sub>oxy</sub>–O2' = 2.29 Å, respectively, and those in trypsin are O2'–Oγ<sub>Ser195</sub> = 2.13 Å, H<sub>2</sub>O<sub>oxy</sub>–Oγ<sub>Ser195</sub> = 2.19 Å, and H<sub>2</sub>O<sub>oxy</sub>–O2' = 2.28 Å, respectively, all well below that of ordinary hydrogen bonds. The crystallographic refinements were performed with the energy terms between the groups involved in the short hydrogen bonds removed. Conventional crystallographic refinement yielded hydrogen bond lengths of between 2.3 and 2.5 Å, but in this instance, the fit of the inhibitor with the well-defined density was noticeably suboptimal in several of the structures. Further characterization regarding the accuracy and the nature of these unusually short hydrogen bonds from crystallographic and mechanistic studies has recently been reported by Katz et al.<sup>14</sup> Upon the basis of these findings it has been proposed that the binding molecule is actually the phenolate ion of the inhibitor over a large range of pH. In thrombin, additional short hydrogen bonds are made among the inhibitor benzimidazole nitrogen (N1), the water trapped in the oxyanion hole, and Oγ<sub>Ser195</sub> (Table 3). In all three enzymes, u-PA, thrombin, and trypsin, there are also more typical length hydrogen bonds involving a distally bound water molecule (H<sub>2</sub>O<sub>distal</sub>), Nε<sub>2His57</sub>, and the backbone nitrogens of Gly193 and Ser195, respectively (Figure 4). Therefore, a complex multicentered network of hydrogen bonds is formed, involving at least three unusually short hydrogen bonds. The X-ray structure of **6b** binding in the active site of u-PA (Figure 3b, i) also reveals a profound effect on the interactions at the bottom of S1 due to the deeper S1 pocket of u-PA compared to trypsin. The amidine group of the inhibitor does not make direct hydrogen bonded salt bridges to Asp189, but rather, a water molecule mediates the interaction between these two groups. To date, all the high-resolution X-ray structures of amidine- or guanidine-bearing inhibitors complexed in the active site of u-PA reveal direct interactions between the inhibitor and Asp189.<sup>6,28</sup> The short and normal range hydrogen bond interactions of the inhibitor **6b** around the Ser195 residue in u-PA are presumably strong enough to compete and perturb the interactions that would normally occur between the amidine group and Asp189. Supportive evidence is also provided by the

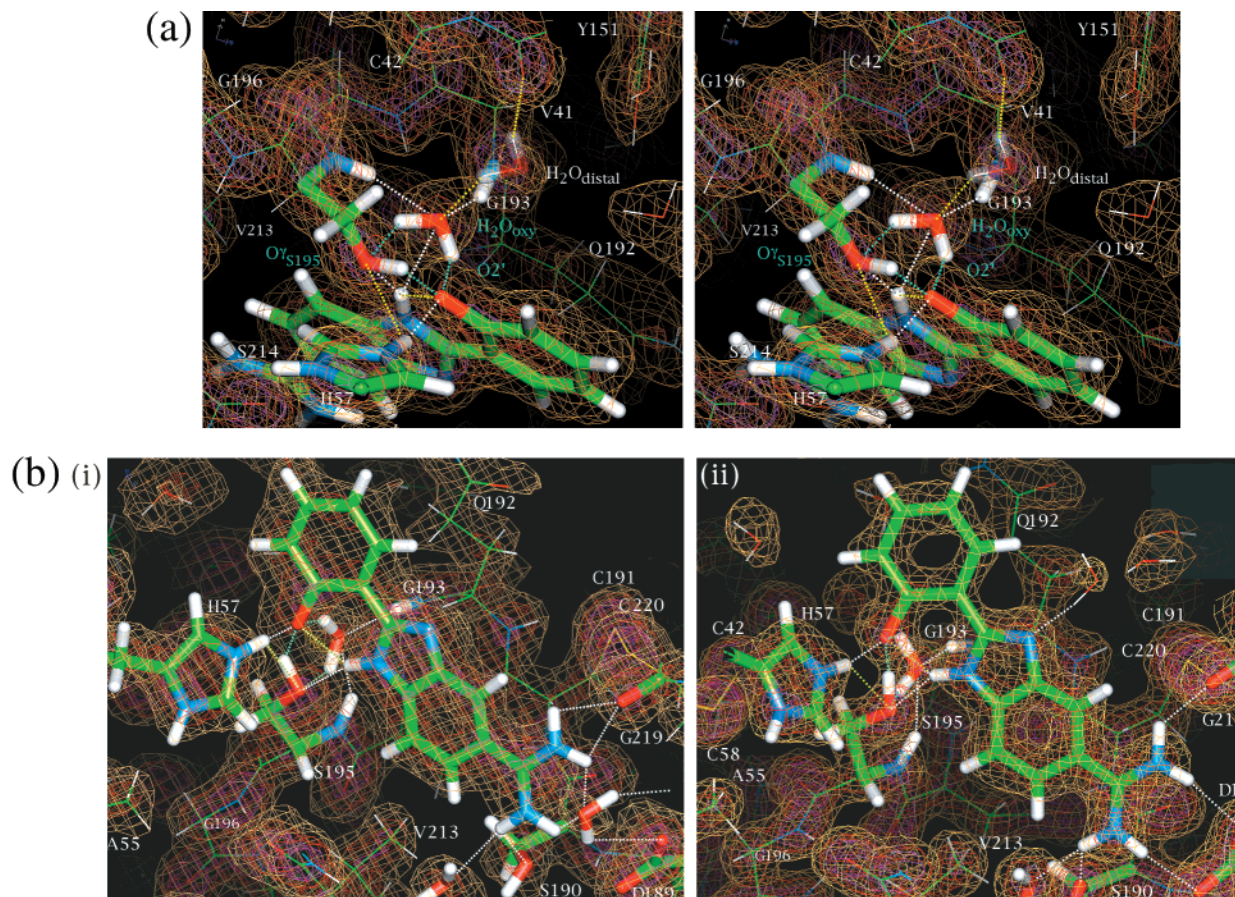


**Figure 3.** (a) Structure and corresponding  $(2|F_o| - |F_c|)$ ,  $\alpha_c$  map contoured at 1.0, 2.4, and 3.8  $\sigma$  for the active site and oxyanion hole of the u-PA-**6b** complex, pH 6.5, 1.75 Å. Short hydrogen bonds are cyan, enzyme-inhibitor and enzyme-water-inhibitor hydrogen bonds white, and intra-enzyme, intra-inhibitor, water-water, and water-enzyme hydrogen bonds yellow. Note that the structure and density for the Cys42 and Cys58 side chains have been removed for clarity. (b) Comparison of density maps of **6b** complexed in (i) u-PA and (ii) trypsin. The short hydrogen bonds are shown as cyan dashed lines, the intra-enzyme or intra-inhibitor hydrogen bonds as yellow dashed lines, and enzyme-water-inhibitor hydrogen bonds as white dashed lines. In part b(i), note the water molecule mediating interactions between the Asp189 residue and the amidine. Another water molecule is also present in the vicinity of Ser190 in both structures and hydrogen bonds to the amidine group.

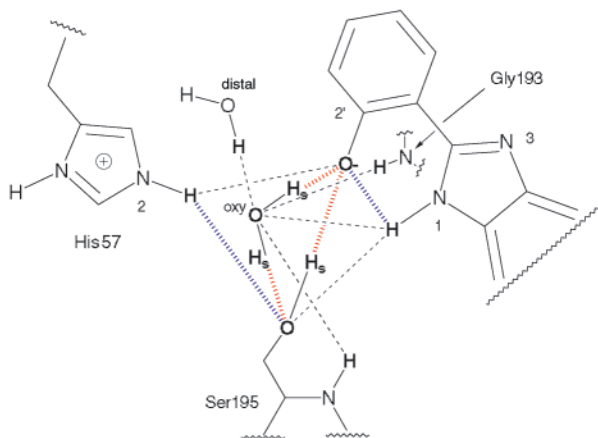


**Figure 4.** Schematic of **6b**, and analogues, binding through short hydrogen bonds to the serine protease Ser195 and His57 residues in trypsin and u-PA. Short hydrogen bonds are shown as red lines. Intra-enzyme and intra-inhibitor hydrogen bonds are shown as blue lines. The hydrogens involved in short hydrogen bonds are denoted as H<sub>s</sub>. The inhibitor hydroxyl group is deprotonated and the enzyme His57 protonated. The hydrogen atoms in bold (H) are also involved in ordinary hydrogen bonds (dashed lines).

X-ray structure of **6a**, a compound which lacks the essential hydroxyl group for forming the network of

short hydrogen bonds. This molecule was found to establish direct interactions with the Asp189 residue (data not shown). Comparison of the assay data between **6a** and **6b** (Table 1) shows that, despite the unfavorable interaction in S1, the introduction of the hydrogen bonding network affords a 10-fold potency enhancement toward u-PA. The structure of trypsin complexed with **6b** (Figure 3b, ii) reveals more typical interactions at the bottom of S1 since the size of the inhibitor is more compatible with the shorter S1 pocket of trypsin compared to u-PA. Surprisingly though, the  $K_i$  value of **6b** compared to **6a** for trypsin indicates only a 2-fold enhancement. These affinity gains for u-PA and especially trypsin are surprisingly small given that there are three new direct hydrogen bonds formed between the inhibitor and the protein and several via H<sub>2</sub>O<sub>oxy</sub>. It is therefore likely that the scaffold is suboptimal due to factors such as, unfavorable van der Waals interactions, desolvation effects, or conformational entropy changes of the inhibitor upon binding.

Initially, substitutions were made around the phenol ring of scaffold **6b** in an attempt to optimize the potency. Given the intricate network of hydrogen bonds between the hydroxyl (phenolate) group of the inhibitor and the enzyme, it was expected that these substitutions affect-



ing the electronic characteristics of this key group might change the inhibition profile for the enzymes. Sterically small substitutions *ortho* to the hydroxyl group **6h–l** (Table 1) were indeed found to have profound effects on potency. In general, the electron withdrawing substitutions, **6h–j** relative to hydrogen, **6b**, tended to give optimal potencies over the electron donating methyl and methoxy substitutions, which resulted in only minor (<3-fold for any enzyme) changes. The bromine substitution, **6j**, caused the greatest increase in affinity toward the entire panel of enzymes except thrombin. The enhancements ranged from 16-fold for trypsin to 47-fold for factor Xa. Affinity toward u-PA was increased 22-fold by the bromine substitution. In the case of thrombin, the nitro group had a slightly greater effect than bromine and gave an additional 2-fold enhancement. Further exploration of larger groups *ortho* to the hydroxyl group resulted in **6m**. Substantial potency enhancements compared to **6b** were noted, but compared to the bromine substitution **6j**, there appears to be no added benefit. It was noticeable that the effects of *ortho* substitution did not correlate in a predictable manner with the relative inductive potentials of the chemical groups. One reason for this is that the group *ortho* to the hydroxyl is directed toward the S1' and therefore introduces additional protein interactions. For example, the aryl ring in **6m** makes contact with the disulfide bridge between Cys42 and Cys58 at the bottom of S1', in addition to interactions with residues His57 and Val41. There is also the likelihood that the close proximity of the *ortho* substituent to the hydrogen bond network also introduces other effects on potency in addition to direct inductive effects.

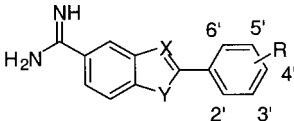
To separate these potential effects from the inductive effects, the same group of substituents, except phenyl, was introduced onto **6b** *para* to the hydroxyl group, examples **6c–g**. This position on the scaffold is directed away from the protein and the hydrogen bond network and toward solvent accessible space. The *para* substitutions **6c–g** had remarkably little effect on affinity toward all the enzymes. The largest change was for the *p*-methoxy analogue, **6g**, which was only marginally (3.5-fold) more potent toward trypsin than lead **6b**. The  $pK_a$  of the phenol group was measured in several of these molecules and found to be 4.25 (nitro, **6c**), 7.88 (fluoro, **6d**), 8.23 (hydrogen, **6b**), and 8.25 (methoxy, **6g**). The lack of a clear correlation between affinity and the relative inductive-electronic effects of the substituents is harder to rationalize in this series of analogues. Clearly other factors in addition to inductive effects must contribute an important role in binding. Recent work has shown that the pH of the assay media can significantly affect the solubility of these analogues in the same media.<sup>14</sup> The benzimidazole group is protonated at low pH and the phenol is deprotonated at high pH, leading to greater solubilities at low and high pH, respectively. Compared to **6b**, the *p*-nitro substituted analogue, **6c**, has a much lower solubility at pH 8.6 (1770-fold lower), whereas the *p*-methoxy analogue, **6g**, is very similar to **6b**. These solubility differences lead to varying free energies of solvation, and consequently varied effects on binding affinity depending on the inhibitor.<sup>14</sup>

Substitution at other sites on the aryl ring has also been explored, but only small changes have been observed. A few examples, analogues **6n–q**, are presented in Table 1. *Meta* substitution or the presence of hydroxyl groups at both C-2' and C-6', compounds **6n–p**, showed no effects on potency. Larger aromatic rings such as naphthyl, **6q**, tended to reduce affinity. *p*-Methyl substitution in addition to *o*-bromo substitution, compound **6r**, gave essentially the same results as compound **6j** with the *o*-bromo substitution alone. Similarly, *p*-chloro substitution in addition to *o*-phenyl substitution, compound **6s**, was very similar to compound **6m** with only *o*-phenyl substitution. These latter results further confirm the lack of effects on affinity at pH = 7.4 by *para* substitutions.

In summary, the SAR performed on the phenolic ring of the molecule yielded compounds **6j** and **6m** as two analogues that display enhanced potency toward the panel of serine proteases. It was apparent that substitution *ortho* to the hydroxyl group had the more dramatic impact on potency whereas substitution around the other sites had only marginal effects on affinity. Attention was now turned to the S1 binding heterocycle part of the molecule.

The 5-amidinobenzimidazole series of analogues **6a–s** occupy the S1 site of the protease as confirmed by X-ray analysis (Figure 3). Using a similar panel of trypsin-like serine protease enzymes, it was reported by Geratz and co-workers that the intrinsic potency of 5-amidinoindole compared to 5-amidinobenzimidazole was between 2- and 350-fold greater.<sup>18</sup> In the case of scaffold **6b**, changing the benzimidazole heterocycle to an indole (compound **19**), thereby fixing the tautomeric nature of the nitrogen compared to the benzimidazole analogues, resulted in at most an 8-fold potency enhancement (Table 2). The lowest enhancement was for u-PA, where activity was only 2-fold greater. However, the same benzimidazole to indole change on the optimized benzimidazole scaffolds **6j** and **6m**, analogues **22b** and **22f**, respectively, resulted in larger potency enhancements. In the case of **22b**, the enhancements were modest and ranged from 5- (trypsin) to 19-fold (thrombin) ultimately resulting in  $K_i$  values below 380 nM toward the whole panel of enzymes. The enhancements increased to 28–50-fold in the case of analogue **22f**. Analogue **22f** has a  $K_i$  toward the whole serine panel of below 320 nM and is the most potent analogue toward u-PA and plasmin. For u-PA, the  $K_i$  = 8 nM is a 50-fold increase over the corresponding benzimidazole analogue, **6m**, and a 700-fold increase over the original lead **6b**. Therefore, the indole ring coupled with the presence of an *ortho* substituted phenol resulted in substantial affinity enhancements across the panel of enzymes. It is unlikely that the larger affinity enhancements in this series of indoles are the result of the proposed greater intrinsic affinity of the 5-amidinoindole compared to 5-amidinobenzimidazole since the comparison of **19** and **6b** reveals only small differences in affinity. Furthermore, the earlier studies<sup>18</sup> reported that there were no intrinsic differences in affinity toward plasmin and trypsin of these two heterocycles which is not consistent with the large enhancements observed for indole **22f** compared to benzimidazole **6m** in this study. An important factor to consider in light of these results is the interaction of



**Table 2.** Effect of Modifications on the S1 Binding Element on Enzyme Inhibition


no.	X	Y	R				formula	$K_i$ ( $\mu$ M)					
			2'	3'	4'	5'		u-PA	t-PA	factor Xa	thrombin	plasmin	trypsin
<b>6b</b>	N	NH	OH	H	H	H	C <sub>14</sub> H <sub>12</sub> N <sub>4</sub> O	5.5	75	14	55	46	23
<b>19</b>	CH	NH	OH	H	H	H	C <sub>15</sub> H <sub>13</sub> N <sub>3</sub> O	2.4	9.4	2.7	13	12	8.0
<b>22a</b>	CH	NH	OH	Br	H	Me	C <sub>16</sub> H <sub>14</sub> BrN <sub>3</sub> O	0.055	0.46	0.052	0.18	0.60	0.32
<b>22b</b>	CH	NH	OH	Br	H	H	C <sub>15</sub> H <sub>12</sub> BrN <sub>3</sub> O	0.035	0.38	0.043	0.12	0.25	0.29
<b>22c</b>	CH	NH	OH	Br	H	Br	C <sub>15</sub> H <sub>11</sub> Br <sub>2</sub> N <sub>3</sub> O	0.10	0.69	0.089	0.32	0.90	1.0
<b>22d</b>	CH	NH	OH	Br	H	NO <sub>2</sub>	C <sub>15</sub> H <sub>11</sub> BrN <sub>4</sub> O <sub>3</sub>	0.28	1.3	0.078	0.24	2.1	4.3
<b>22e</b>	CH	NH	OH	Ph	H	Me	C <sub>22</sub> H <sub>19</sub> N <sub>3</sub> O	0.038	0.11	0.21	1.1	0.25	0.13
<b>22f</b>	CH	NH	OH	Ph	H	H	C <sub>21</sub> H <sub>17</sub> N <sub>3</sub> O	0.008	0.035	0.078	0.32	0.10	0.13
<b>22g</b>	CH	NH	OH	Ph	H	Br	C <sub>21</sub> H <sub>16</sub> BrN <sub>3</sub> O	0.043	0.094	0.21	1.4	0.35	0.70
<b>22h</b>	CH	NH	OH	Ph	H	Cl	C <sub>21</sub> H <sub>16</sub> ClN <sub>3</sub> O	0.055	0.16	0.34	0.29	0.29	0.13
<b>22i</b>	CH	NH	OH	Ph	H	NO <sub>2</sub>	C <sub>21</sub> H <sub>16</sub> N <sub>4</sub> O <sub>3</sub>	0.025	0.019	0.014	0.11	0.19	0.075
<b>22j</b>	CH	NH	H	Ph	H	H	C <sub>21</sub> H <sub>17</sub> N <sub>3</sub>	13	138	43	32	26	17
<b>22k</b>	CH	NH	OMe	Ph	H	H	C <sub>22</sub> H <sub>19</sub> N <sub>3</sub> O	3.2	19	19	22	26	1.2
<b>49</b>	NMe	N	OH	Ph	H	H	C <sub>21</sub> H <sub>18</sub> N <sub>4</sub> O	11	150	30	70	12	6.5
<b>58</b>	CH	O	OH	Ph	H	H	C <sub>21</sub> H <sub>16</sub> N <sub>2</sub> O <sub>2</sub>	0.55	2.8	6.8	7.0	5.5	1.6

**Table 3.** Enzyme–Inhibitor and Enzyme–H<sub>2</sub>O<sub>oxy</sub>–Inhibitor Hydrogen Bond Lengths at the Active Sites of Trypsin, Thrombin, and u-PA Complexes of **6b** and Analogues<sup>a</sup>

complex	pH	O2'–O <sub>γ</sub> Ser195	H <sub>2</sub> O <sub>oxy</sub> –O <sub>γ</sub> Ser195	H <sub>2</sub> O <sub>oxy</sub> –O2'	H <sub>2</sub> O <sub>oxy</sub> –N1	O <sub>γ</sub> Ser195–N1	Ne2His57–O2'
u-PA							
<b>6b</b> <sup>b</sup>	6.50	2.14 (14)	2.30 (12)	2.29 (08)	2.77(08)	2.63 (04)	2.68 (04)
<b>22f</b> <sup>c</sup>	6.50	2.33	2.22	2.33	2.95	2.72	2.70
<b>22a</b> <sup>d</sup>	6.50	2.00	2.39	2.21	2.87	2.51	2.69
Trypsin							
<b>6b</b>	3.50–9.45	2.13 (07)	2.19 (11)	2.28 (06)	2.57 (11)	2.58 (07)	2.67 (05)
<b>22f</b>	7.07	2.01	2.27	2.31	2.85	2.63	2.75
<b>22a</b>	8.00	2.29	2.08	2.39	2.83	3.02	2.71
Thrombin							
<b>6b</b>	5.34–8.28	2.26 (19)	2.26 (19)	2.35 (15)	2.37 (13)	2.46 (05)	2.70 (05)
<b>22a</b>	7.80	2.08	2.27	2.17	2.39	2.42	2.89

<sup>a</sup> O2' is the inhibitor hydroxyl oxygen. N1 is the nitrogen of the benzimidazole proximal to the Ser195 residue. H<sub>2</sub>O<sub>oxy</sub> is the water in the oxyanion hole. Ne2His57 is the proximal nitrogen of the catalytic His57 residue. O<sub>γ</sub>Ser195 is the oxygen of the Ser195 hydroxyl group. For further direction, see Figure 3. Standard deviations are in parentheses. <sup>b</sup> Resolution = 1.75 Å; *R* = 20.5%. <sup>c</sup> Resolution = 1.73 Å; *R* = 20.2%. <sup>d</sup> Resolution = 1.65 Å; *R* = 24.4%.

the S1 binding heterocycle with the intricate network of hydrogen bonds. On the basis of the binding mode determined for **6b**, the nitrogen atom N1 donates a hydrogen bond to O<sub>γ</sub>Ser195 and the water molecule in the oxyanion hole thereby affording some stabilization. The indole nitrogen has fixed hydrogen bond donating character, but in contrast, the benzimidazole has two possible tautomers, only one of which is the preferred binding conformer (N1 protonated). Gas phase energy calculations on **6b** have indicated that this molecule is more stable in the unfavorable tautomer conformation relative to the mode of binding.<sup>14</sup> It seems reasonable to postulate that this tautomeric ambiguity leads to the weaker affinities of the benzimidazoles compared to indoles in this series of analogues, e.g., **6m** compared to **22f**, and **6r** compared to **22a**. Consequently, on the basis of this theory it would be expected that N3 substituted benzimidazoles, e.g., **49**, that have a fixed, unfavorable tautomeric state relative to the preferred binding mode, would be poor inhibitors. To this end, compound **49** (Table 2) can be directly compared to the unsubstituted benzimidazole **6m** and indole **22f**. The potency of **49** is consistently lower than the benzimidazole analogue **6m** across the whole panel of enzymes except trypsin, and **6m** is itself consistently less active

than indole **22f** for all enzymes. Assuming that the additional methyl group was not significantly changing other binding factors, this result supports the proposed theory. Furthermore, the benzofuran analogue of **22f**, analogue **58**, which cannot donate a hydrogen bond, in general, displayed a similar affinity profile to that of **6m**. Although these results need further investigation, they strongly suggest that a hydrogen bond donor is necessary at this position of the scaffold for optimal affinity.

The scaffolds **22b** (*o*-bromo) and **22f** (*o*-phenyl) were substituted at the *para* position to create two series of analogues, **22a–d** and **22e–i**, respectively (Table 2). Comparing and contrasting the effects on affinity of *para* substitution on the indole scaffolds to those observed on the benzimidazole scaffolds reveals a subtle difference. In the benzimidazole series, **6b–g**, *para* substitution resulted in potency fluctuations of no more than 3.5-fold between the most and least potent analogues. However, *para* substitutions on the *o*-phenyl scaffold, analogues **22e–i**, resulted in more significant potency fluctuations. For example, comparing the factor Xa affinity for **22h** (*p*-chloro) with **22i** (*p*-nitro) indicates a 24-fold change in potency (Table 2). In the *o*-bromo indole analogues **22a–d**, the fluctuations were greatest

toward trypsin where the potency changed by 15-fold between **22b** and **22d**. Despite this difference in sensitivity toward *para* substitution, there is still no clear correlation with the relative inductive effects of the substitutions at the *para* position in either the *o*-bromo or *o*-phenyl series at pH = 7.4, presumably for reasons similar to those mentioned earlier. A striking example of this is the fact that *p*-nitro analogue in the *o*-phenyl series, compound **22i**, has optimal potency toward t-PA and trypsin within that series, but the same *p*-nitro substitution on the *o*-bromo series, **22d**, leads to the lowest comparative potency toward t-PA, trypsin, plasmin, and u-PA. The analogue **22i** is the most potent inhibitor shown for t-PA, factor Xa, thrombin, and trypsin displaying a  $K_i$  below 190 nM across the whole panel of enzymes.

To establish the necessity of the hydroxyl group toward binding in some of the potent inhibitors such as **22f**, compound **22j** (the analogue of **22f** without the hydroxyl group) was prepared. Analogue **22j** was significantly less potent than **22f** toward all the enzymes and was also less potent than **19**, the basic indole scaffold with no *ortho* substitution. The masking of the hydroxyl group as a methyl ether, compound **22k**, also afforded a reduction in potency across the whole panel. Removal of the basic amidine group also leads to significantly poorer inhibition across all the enzymes in the panel (data not shown). These results, taken together, indicate that the interactions between the basic group of the inhibitor and Asp189 in the S1 subsite, and the interactions of the hydroxyl group with the catalytic residues, are both essential components of binding for these inhibitors.

The optimized indole scaffolds **22a** and **22f** do not show affinity enhancements toward any of the enzymes in the presence of free zinc ions (data not shown). This result was expected, since the indole scaffold is a weaker zinc chelator compared to the benzimidazole scaffold. Zinc-mediated binding modes are possible for the benzimidazoles **6c–s** as discovered earlier for **6b**.<sup>14</sup> However, at pH = 7.4, the optimal benzimidazole based inhibitors, **6r** and **6m**, displayed only small (10–20-fold) affinity shifts in the presence of free zinc ions, much lower than the 5 orders of magnitude found for the BABIM-type<sup>1,12</sup> compounds (see Supporting Information). Therefore it is unlikely that the zinc-mediated binding modes of these inhibitors will contribute toward inhibitor potency under physiological conditions.

Given the successful optimization of the lead **6b** into several broadly potent zinc-independent inhibitors (**22a–b**, **22f**, **22h–i**), it was necessary to confirm that the mode of binding was similar to that of **6b** and that the affinity enhancements were not the result of an entirely different binding mode. From the *o*-bromo series, **22a** was chosen, and from the *o*-phenyl series, **22f**, since both had good generic potency profiles but were also highly potent for two targets of particular interest to this group, u-PA and factor Xa respectively. Figure 5a shows a stereoview density map of inhibitor **22f** bound in the active site of u-PA at 1.7 Å resolution. The inhibitor is well-ordered, and a water molecule, trapped in the oxyanion hole, sits in close proximity to the inhibitor hydroxyl oxygen and the Ser195 hydroxyl oxygen. The hydrogen-bonding distances between the oxygen atoms

are all shorter than ordinary hydrogen bond lengths and therefore similar to that of the u-PA-**6b** complex (Table 3). Also clearly visible in the density map are two water molecules in the S1 subsite of u-PA, one mediating binding from the amidine to Asp189, the other participating in hydrogen bonding with the amidine group. Both of these water molecules can be found in the corresponding complex of **6b** in u-PA. The aryl group, as noted above, is directed toward S1' and makes van der Waals contact with the disulfide bridge between Cys42 and Cys58, His57 and Val41. Figure 5b shows the overlaid structures of **22f** and **6b** in u-PA at pH = 6.5, and Figure 5c the overlay of the two inhibitors in trypsin at pH = 7.1 and 6.4, respectively. Essentially the molecules bind in identical modes in both enzymes, and the key short hydrogen bonding distances compare very nicely (Table 3). The most significant difference to note is the small shift of residue His57 in the complexes of **22f**. The histidine is most likely protonated at the pH of crystallization (pH = 6.5) and presumably moves to interact favorably with the aryl ring of **22f**. The affinity of **22f** was measured at pH = 6.5 under conditions identical to those of the crystallization process, and only minor (<2-fold) differences were observed compared to the affinities measured at pH 7.4 (data not shown). Thus, the dramatic potency enhancements of **22f** in u-PA (700-fold) and trypsin (177-fold) compared to **6b** are not the result of gross changes in the binding mode.

A similar structural analysis was performed for **22a**, whose affinity enhancements over **6b** ranged from 72-fold (trypsin) to 269-fold (factor Xa). The density map of **22a** complexed in u-PA (Figure 6a) is very comparable to that of **6b** complexed in u-PA (Figure 3b, i) and therefore, by default, **22f**. The complex displays the expected pattern of short hydrogen bonds with the inhibitor being well ordered and co-binding with the two water molecules in S1. The distance between O2' and O<sub>γ</sub>Ser195 is very short, only 2.00 Å, well below a typical hydrogen bond distance of 2.6 Å. Figure 6b shows the overlay of **6b** and **22a** in thrombin and, similar to **22f**, reveals an identical binding mode for the two inhibitors. The indole nitrogen engages in short hydrogen bonds with O<sub>γ</sub>Ser195 and the H<sub>2</sub>O<sub>oxy</sub> as observed for the inhibitor **6b** in thrombin. Table 3 reflects these observations but also indicates that the largest differences occur between the complexes of **22a** and **6b** in trypsin, whereby the O<sub>γ</sub>Ser195–N1 (benzimidazole nitrogen) distance is 0.4 Å longer. An overlay of these inhibitors in trypsin is shown in Figure 6c. The inhibitor **22a** has moved away from the catalytic residues slightly and sinks deeper into the S1 pocket, thus lengthening the hydrogen bond from the nitrogen of the inhibitor to the Ser195 residue. The hydrogen bonds involving the triangle of oxygens remain short, however, since the water molecule in the oxyanion hole also moves slightly. Despite these changes, the overall structures are still very similar. In addition to the structures presented here, many other high-resolution structures of inhibitors from this class of scaffold, complexed with different serine proteases, have displayed similar modes of binding involving short hydrogen bonds.<sup>14</sup> On the basis of this evidence, the tighter binding observed in the optimized inhibitors such as **22f** and **22a** cannot be

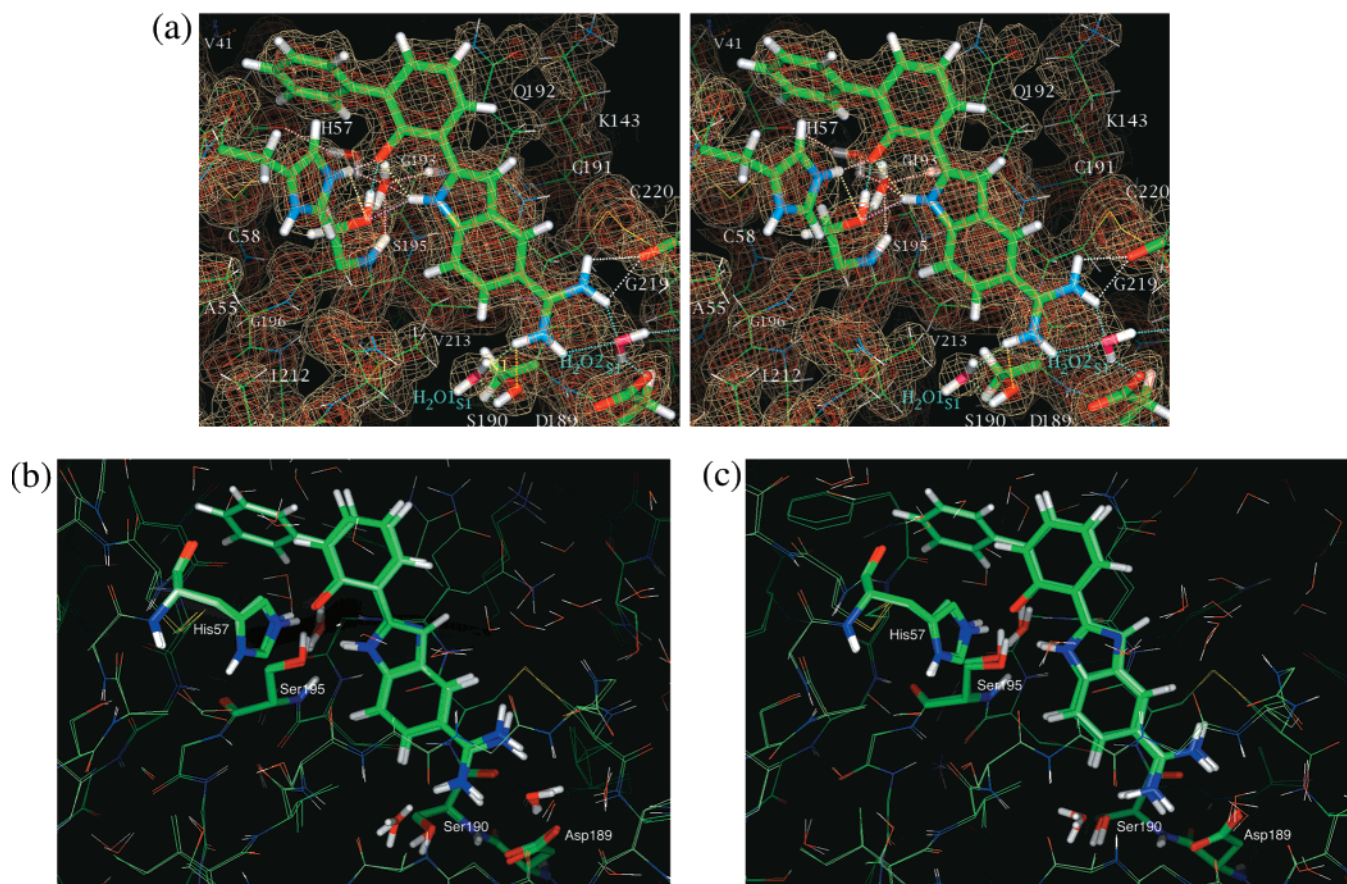


**Figure 5.** (a) Stereoview of **22f** complexed in the active site of u-PA. The color coding of the hydrogen bonds (dashed lines) near the catalytic residues is the same as for Figure 3 except the enzyme–water–inhibitor hydrogen bonds are in magenta. Hydrogen bonds involving H<sub>2</sub>O<sub>S1</sub> are shown in cyan and those involving H<sub>2</sub>O<sub>S1</sub>, Ser190, and the inhibitor are in green and yellow. (b) Overlay of the u-PA structures of **6b** and **22f** at pH = 6.5. (c) Overlay of the trypsin structures of **6b** and **22f** at pH = 6.4 and pH = 7.1, respectively. Both overlays show the very close (almost identical) binding modes of the two inhibitors in each enzyme. In part b, a water molecule mediates the interaction between Asp189 and the amidine in both structures and is absent in part c. The aryl group of **22f** is directed toward S1'.

rationalized through gross changes in the binding mode. These inhibitors therefore represent optimized inhibitors for this binding mode involving short and normal range hydrogen bonds.

The cumulative SAR data and structural information presented suggests that four factors contribute to the overall potency of these new inhibitors. First, the phenolic group that is involved in an elaborate network of short and normal range hydrogen bonds, second a basic group to interact either directly or indirectly with the Asp189 residue, third *ortho* substitution to the phenol, and finally an S1 heterocycle bearing the appropriate NH functionality. The first three of these four key functional groups are all essential for optimal binding, and removal of any one will cause a dramatic reduction in potency. For this reason, it is extremely difficult to separate the individual effects on binding affinity of these four factors from the overall binding affinity in order to estimate the contribution from the hydrogen bond network alone. However, by comparing two inhibitors that differ only in the length of the hydrogen bonds formed at the active site in thrombin, the contribution of the short hydrogen bonds over the normal range hydrogen bonds was estimated to be in the range of up to 1.7 kcal/mol.<sup>14</sup> This relatively small increase means that the formation of the unusually short hydrogen bonds is unlikely to be the major

contributor to the large potency enhancements in these optimized inhibitors. Rather, it is more likely that the affinity enhancements of inhibitors **22f** and **22a**, for example, are due to the combination of both the short and normal range hydrogen bonds and other factors, such as the aforementioned inductive effects, free energies of solvation, and van der Waals interactions.

A key question regarding the potential of these generic inhibitors for drug development that has not been addressed relates to the possibility of engineering selectivity onto the scaffolds. Due to the two key binding elements, the basic group and the multicentered network of hydrogen bonds interacting with Ser195, it is unlikely that enzymes other than trypsin-like serine proteases would be targeted by such molecules. The critical enzymes that then remain as antitargets would only be those members of the trypsin-like serine proteases that are closely related to the target of interest, for instance, t-PA if one were targeting u-PA. In the data shown for the most potent analogues, there are some hints of selectivity for one enzyme over another even though the inhibitors are largely unelaborated. It is worth noting that these inhibitors are relatively rigid and possess very few rotatable bonds. The combination of these properties with the strong 2-fold 'anchorage' of the inhibitors results in a strong dependence of affinity on substituents placed around the scaffold. Appending



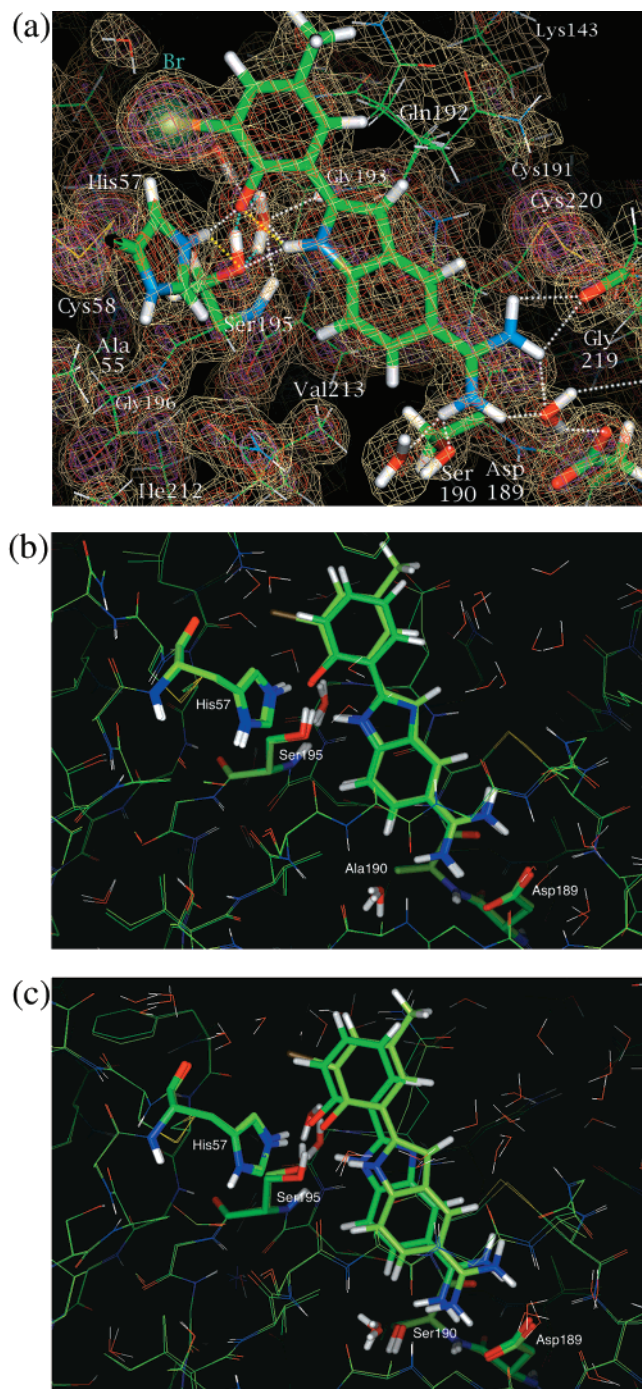


**Figure 6.** (a) **22a** complexed in the active site of u-PA at pH = 6.5. The color coding of the hydrogen bonds (dashed lines) near the catalytic residues are the same as for Figure 3. (b) Overlay of the **22a** and **6b** complexes in thrombin at pH = 7.8. The complexes are almost identical with the bromine of **22a** directed toward the S1' pocket and the *para* methyl group toward solvent. (c) Overlay of the **22a** and **6b** complexes in trypsin at pH = 8.0 and pH = 6.4, respectively. The complexes in this case show the most dramatic differences. The inhibitor **22a** relative to **6b** sits deeper into the S1 pocket extending the length of the N1–O $\gamma$ <sub>Ser195</sub> and N1–H $_2$ O<sub>oxy</sub> hydrogen bonds and is tilted away from the catalytic residues slightly. The short hydrogen bonds are maintained between the O2'–O $\gamma$ <sub>Ser195</sub>, O2'–H $_2$ O<sub>oxy</sub>, and O $\gamma$ <sub>Ser195</sub>–H $_2$ O<sub>oxy</sub>.

groups onto the S1 binding heterocycle or *para* to the phenol group has been found to decrease affinity toward some enzymes while enhancing affinity toward others. For example, earlier work using small S1 binding

molecules of the serine proteases identified subtle differences within the S1 pocket such as the identity of residue 190 that can be exploited for the generation of selectivity.<sup>28a</sup> The enzymes, despite being highly homologous in this region, do tend to have their own unique characteristics or 'fingerprint'. Efforts to apply this knowledge onto **22f** have led to the development of highly selective inhibitors of u-PA through subtle modifications of the S1 binding group (manuscript in preparation). Furthermore, substitution at the 3-position of the indole ring was found to enhance affinity toward factor Xa but reduce affinity toward u-PA, t-PA, plasmin, and trypsin thereby generating selective factor Xa inhibitors.<sup>15</sup>

## Conclusion

The screening lead **6b** has the unique property of being able to bind to serine proteases in two distinct and unique binding modes, one zinc-dependent the other zinc-independent. The zinc-independent binding mode comprises a multicentered network of short and normal range hydrogen bonds. Potency optimization through subtle chemical modifications has yielded several inhibitors (**22a**, **22b**, **22f**, **22i**) that display  $K_i$  values below 600 nM toward a panel of six human serine proteases including important targets such as u-PA and factor Xa. The binding mode for the optimized inhibitors has also been demonstrated to involve an almost identical network of short and normal range hydrogen bonds involving the hydroxyl group of the inhibitor, the catalytic serine, and a water molecule trapped in the oxyanion hole. These interactions form the basis of a fully reversible and unique 'anchor' point to the protein. The basic amidine group interacting with Asp189 at the bottom of the S1 pocket, either directly or indirectly through a water molecule, provides a second 'anchor' point. These key 'anchor' points between the inhibitor and protein coupled with the commonality of the key protein residues that are involved affords inhibitors or scaffolds that are inherently potent toward a whole family of enzymes. Removal of groups on the inhibitor that contribute to these noncovalent interactions around the catalytic residues and van der Waals contacts in S1' results in sharply decreasing potency. The two inhibitors **22a** and **22f**, both developed through relatively minor modifications from the original lead **6b**, have displayed enhancements in potency of up to 2000-fold over **6b**. These novel inhibitors are now serving as leads in drug discovery efforts toward the development of selective and orally available u-PA, factor Xa, and factor VIIa inhibitors. The availability of high resolution crystal structures of these inhibitors complexed in u-PA and other targets has provided unique opportunities for engineering selectivity into the molecules. This, together with the fully reversible binding mode, the relative synthetic accessibility, and nonpeptidic nature of the molecules provides a nice platform for rapidly developing therapeutically useful molecules for a variety of protease targets.

## Experimental Section

Reactions were carried out under an inert atmosphere at room temperature unless indicated otherwise. Solvents and chemicals were reagent grade or better and were obtained from commercial sources. All aldehyde, acetophenone, and benzoic

acid reagents were obtained from commercial sources unless otherwise indicated. Silica gel chromatography was performed using Merck Kieselgel 60 (230–400 Mesh). Preparative HPLC purification was carried out on a Gilson HPLC fitted with a VYDAC C18 (5 × 25 cm) column eluting at 50 mL/min with a gradient of 2–90% solvent B in solvent A over 60 min (solvent A was 20 mmol aqueous HCl and solvent B was CH<sub>3</sub>CN, or solvent A was 0.1% TFA in water and solvent B 0.1% TFA in CH<sub>3</sub>CN). Analytical HPLC analysis was performed using a HP1100 eluting with a gradient of 2–90% solvent B in solvent A (solvent A was 0.05% TFA in water and solvent B was CH<sub>3</sub>CN). NMR spectroscopy was determined on a GE 300 MHz NMR fitted with a 300/44 5 mm <sup>31</sup>P-<sup>15</sup>N/<sup>1</sup>H probe or a JEOL ECLIPSE 270 MHz NMR. Chemical shifts are reported in units of  $\delta$  (ppm) and peak multiplicities are expressed as follows: s, singlet; d, doublet; t, triplet; br, broad peak; q, quartet; m, multiplet; dd, doublet of doublet; ddd, doublet of doublet of doublets. Mass spectra were determined on a Perkin-Elmer Sciex API-150EX mass spectrometer equipped with a turbo ion spray source (MS-Sciex) or a Finnigan TSQ7000 equipped with ElectroSpray ionization source (MS-ESI). The analytical microanalysis were carried out by Robertson Microlit Laboratories Inc., Madison, NJ, and were within 0.4% units of the theoretical values unless otherwise indicated.

**3,4-Diaminobenzamidine Dihydrochloride (5).** This compound was prepared by the procedure of Fairley et al.<sup>17</sup>

Compounds **6a–s** were made using one of the general procedures A–D shown below.

**General Procedure A: Example, 2-(2-Hydroxy-5-methylphenyl)-1H-benzimidazole-5-carboxamide (6f).** A suspension of 3,4-diaminobenzamidine dihydrochloride **5** (150 mg, 0.67 mmol) in absolute EtOH (10 mL) at 90 °C was treated over 2 min with a solution of 2-hydroxy-5-methylbenzaldehyde **12** (91 mg, 0.67 mmol) in absolute EtOH (2 mL). The mixture was heated for 2–3 h, and the solution was then allowed to cool. Et<sub>2</sub>O was added, and the precipitate that formed was collected by filtration. The precipitate was subjected to reverse phase HPLC to give **6f** (yields typically ranged from 10 to 50% for the analogues presented). <sup>1</sup>H NMR (DMSO-*d*<sub>6</sub>)  $\delta$  9.56 (br s, 2H), 9.29 (br s, 2H), 8.27 (s, 1H), 8.18 (s, 1H), 7.96 (d, *J* = 8.4 Hz, 1H), 7.85 (dd, *J* = 8.6, 1.5 Hz, 1H), 7.34 (dd, *J* = 8.4, 1.8 Hz, 1H), 7.16 (d, *J* = 8.5 Hz, 1H), 2.32 (s, 3H). <sup>13</sup>C NMR (DMSO-*d*<sub>6</sub>)  $\delta$  165.8, 155.8, 151.6, 137.2, 137.1, 135.0, 134.0, 128.5, 124.0, 123.6, 117.2, 115.3, 114.6, 109.9, 20.0. MS-Sciex *m/z* 266.8 [MH<sup>+</sup>]. Anal. (C<sub>15</sub>H<sub>14</sub>N<sub>4</sub>O·1.5HCl·0.75H<sub>2</sub>O) C, H, N.

**General Procedure B: Example, 2-(2-Hydroxy-3-bromophenyl)-1H-benzimidazole-5-carboxamide (6j).** 3,4-Diaminobenzamidine dihydrochloride **5** (0.23 g, 1.24 mmol) was added to *N,N*-dimethylacetamide (6 mL) followed by Na<sub>2</sub>S<sub>2</sub>O<sub>5</sub> (0.31 g, 1.62 mmol) and finally 3-bromo-2-hydroxybenzaldehyde **8** (0.25 g, 1.24 mmol). The resultant mixture was heated at 100 °C for 3 h and then allowed to cool. Et<sub>2</sub>O (200 mL) was added, and the solution was stirred overnight. The precipitate that formed was collected by filtration, washed with cold Et<sub>2</sub>O, and dried to give a crude solid (0.62 g). Half of the solid was subjected to preparative HPLC to give **6j** (50 mg, 11%, 22% based on crude solid weight). <sup>1</sup>H NMR (DMSO-*d*<sub>6</sub>)  $\delta$  9.44 (br s, 2H), 9.16 (br s, 2H), 8.31–8.25 (m, 2H), 7.88 (d, *J* = 8.6 Hz, 1H), 7.79–7.74 (m, 2H), 7.02 (t, *J* = 8.4 Hz, 1H). <sup>13</sup>C NMR (DMSO-*d*<sub>6</sub>)  $\delta$  165.8, 154.9, 153.7, 135.6, 126.4, 123.0, 122.4, 120.4, 113.2, 110.7. MS-Sciex *m/z* 331.0 [<sup>79</sup>Br, MH<sup>+</sup>], 333.0 [<sup>81</sup>Br, MH<sup>+</sup>]. Anal. (C<sub>14</sub>H<sub>11</sub>BrN<sub>4</sub>O·HCl·0.5H<sub>2</sub>O) C, H, N.

**General Procedure C: Example, 2-(2-Hydroxy-3-fluorophenyl)-1H-benzimidazole-5-carboxamide (6i).** 3,4-Diaminobenzamidine dihydrochloride **5** (1.43 g, 7.7 mmol) was added to absolute EtOH (50 mL) followed by 3-fluoro-2-hydroxybenzaldehyde (1.07 g, 7.7 mmol) and 1,4-benzoquinone (0.83 g, 7.7 mmol). The resultant mixture was heated at reflux for 4 h and then allowed to cool. The solvent was removed under reduced pressure, and the resultant crude solid was subjected to preparative HPLC to give **6i** (2.34 g, 89%). <sup>1</sup>H NMR (DMSO-*d*<sub>6</sub>)  $\delta$  9.60 (br s, 2H), 9.34 (br s, 2H), 8.28 (d, *J* = 1.7 Hz, 1H), 8.16 (d, *J* = 8.8 Hz, 1H), 7.92 (d, *J* = 9.6 Hz,

1H), 7.83 (dd, *J* = 9.6, 1.9 Hz, 1H), 7.45 (m, 1H), 7.04 (m, 1H). <sup>13</sup>C NMR (DMSO-*d*<sub>6</sub>)  $\delta$  165.9, 152.5, 151.5 (d, *J* = 267 Hz), 146.2 (d, *J* = 16.6 Hz), 137.8, 134.9, 124.0, 123.8, 123.4, 119.4–119.7 (2 × C, m), 119.5 (d, *J* = 5.2 Hz), 115.9, 114.7, 113.5 (d, *J* = 4.0 Hz). MS-Sciex *m/z* 271.2 [MH<sup>+</sup>]. Anal. (C<sub>14</sub>H<sub>11</sub>FN<sub>4</sub>O·2.0HCl) C, H, N.

**General Procedure D: Example, 2-(2-Hydroxy-3-methylphenyl)-1H-benzimidazole-5-carboxamide (6k).** 3,4-Diaminobenzamidine dihydrochloride **5** (0.35 g, 1.57 mmol) was added to polyphosphoric acid (PPA) (8 mL) followed by 3-methylsalicylic acid (0.24 g, 1.57 mmol). The mixture was stirred and heated to 180 °C. Analytical HPLC was used to determine completion of the reaction which was typically between 2 and 3 h. The mixture was treated with ice water and neutralized to pH = 7.0 with NH<sub>4</sub>OH solution. The precipitate that formed was collected by filtration and suspended in water. The insoluble material was collected by filtration and dried. The crude solid was subjected to preparative HPLC to give **6k** (90 mg, 19%). Yields were typically in the 10–30% range. <sup>1</sup>H NMR (DMSO-*d*<sub>6</sub>)  $\delta$  9.43 (br s, 2H), 9.18 (br s, 2H), 8.20 (s, 1H), 8.07 (d, *J* = 7.7 Hz, 1H), 7.83 (d, *J* = 8.4 Hz, 1H), 7.74 (d, *J* = 8.8 Hz, 1H), 7.31 (d, *J* = 7.3 Hz, 1H), 6.93 (t, *J* = 7.3 Hz, 1H), 2.24 (s, 3H). <sup>13</sup>C NMR (DMSO-*d*<sub>6</sub>)  $\delta$  165.9, 156.5, 154.5, 133.6, 125.9, 124.8, 122.9, 122.2, 118.9, 115.7, 114.3, 111.1, 15.8. MS-Sciex *m/z* 266.8 [MH<sup>+</sup>]. Anal. (C<sub>15</sub>H<sub>14</sub>N<sub>4</sub>O·1.5HCl·0.25H<sub>2</sub>O) C, H, N.

**2-Phenyl-1H-benzimidazole-5-carboxamide (6a).** Synthesized using general procedure A. <sup>1</sup>H NMR (DMSO-*d*<sub>6</sub>)  $\delta$  9.59 (br s, 2H), 9.30 (br s, 2H), 8.47 (d, *J* = 6.3 Hz, 1H), 8.45 (d, *J* = 8.5 Hz, 1H), 8.28 (d, *J* = 1.1 Hz, 1H), 7.95 (d, *J* = 9.4 Hz, 1H), 7.86 (dd, *J* = 9.6, 1.7 Hz, 1H), 7.70–7.66 (m, 3H). <sup>13</sup>C NMR (DMSO-*d*<sub>6</sub>)  $\delta$  165.7, 152.5, 138.2, 135.0, 132.6, 129.4, 128.0, 125.6, 124.1, 123.6, 115.5, 114.6. MS-Sciex *m/z* 237.0 [MH<sup>+</sup>]. Anal. (C<sub>14</sub>H<sub>12</sub>N<sub>4</sub>·2.0HCl) C, H, N.

**2-(2-Hydroxyphenyl)-1H-benzimidazole-5-carboxamide (6b).** Synthesized using general procedure A. <sup>1</sup>H NMR (DMSO-*d*<sub>6</sub>)  $\delta$  9.49 (br s, 2H), 9.21 (br s, 2H), 8.29 (d, *J* = 7.3 Hz, 1H), 8.23 (s, 1H), 7.93 (d, *J* = 8.4 Hz, 1H), 7.79 (d, *J* = 8.8 Hz, 1H), 7.49 (t, *J* = 7.7 Hz, 1H), 7.21 (d, *J* = 8.1 Hz, 1H), 7.06 (t, *J* = 7.4 Hz, 1H). <sup>13</sup>C NMR (DMSO-*d*<sub>6</sub>)  $\delta$  165.8, 157.9, 151.4, 136.9, 134.3, 133.8, 128.8, 124.1, 123.7, 119.7, 117.3, 115.3, 114.5, 110.2. MS-Sciex *m/z* 253.0 [MH<sup>+</sup>]. Anal. (C<sub>14</sub>H<sub>12</sub>N<sub>4</sub>O·2.0HCl) C, H, N.

**2-(2-Hydroxy-5-nitrophenyl)-1H-benzimidazole-5-carboxamide (6c).** Synthesized using general procedure A. <sup>1</sup>H NMR (DMSO-*d*<sub>6</sub>)  $\delta$  9.51 (br s, 2H), 9.25 (br s, 2H), 9.19 (d, *J* = 2.6 Hz, 1H), 8.32–8.27 (m, 2H), 7.92 (d, *J* = 8.4 Hz, 1H), 7.79 (d, *J* = 8.4 Hz, 1H), 7.39 (d, *J* = 9.2 Hz, 1H). <sup>13</sup>C NMR (DMSO-*d*<sub>6</sub>)  $\delta$  165.9, 163.2, 151.0, 139.8, 138.8, 135.9, 128.1, 124.7, 123.6, 123.1, 118.2, 116.2, 115.0, 112.3. MS-Sciex *m/z* 297.8 [MH<sup>+</sup>]. Anal. (C<sub>14</sub>H<sub>11</sub>N<sub>5</sub>O<sub>3</sub>·2.0HCl) C, H, N.

**2-(2-Hydroxy-5-fluorophenyl)-1H-benzimidazole-5-carboxamide (6d).** Synthesized using general procedure D. <sup>1</sup>H NMR (DMSO-*d*<sub>6</sub>)  $\delta$  9.56 (br s, 2H), 9.29 (br s, 2H), 8.29–8.25 (m, 3H), 7.94 (dd, *J* = 8.4, 3.3 Hz, 1H), 7.84–7.80 (m, 1H), 7.42–7.35 (m, 1H), 7.30–7.24 (m, 1H). <sup>13</sup>C NMR (DMSO-*d*<sub>6</sub>)  $\delta$  153.4, 142.7 (d, *J* = 234 Hz), 142.0, 138.2, 124.8, 121.7, 111.8, 111.4, 108.7 (d, *J* = 23 Hz), 106.4 (d, *J* = 7.3 Hz), 103.2, 102.4, 101.9 (d, *J* = 26 Hz), 98.5 (d, *J* = 8.5 Hz). MS-Sciex *m/z* 271.0 [MH<sup>+</sup>]. Anal. (C<sub>14</sub>H<sub>11</sub>FN<sub>4</sub>O·1.5HCl·0.5H<sub>2</sub>O) C, H, N, F.

**2-(2-Hydroxy-5-bromophenyl)-1H-benzimidazole-5-carboxamide (6e).** Synthesized using general procedure D. <sup>1</sup>H NMR (DMSO-*d*<sub>6</sub>)  $\delta$  9.54 (br s, 2H), 9.28 (br s, 2H), 8.54 (d, *J* = 2.5 Hz, 1H), 8.28 (s, 1H), 7.95 (d, *J* = 8.7 Hz, 1H), 7.83 (dd, *J* = 8.7, 1.5 Hz, 1H), 7.64 (dd, *J* = 8.9, 2.5 Hz, 1H), 7.22 (d, *J* = 8.9 Hz, 1H). <sup>13</sup>C NMR (DMSO-*d*<sub>6</sub>)  $\delta$  165.8, 157.1, 150.8, 137.8, 136.0, 134.7, 130.5, 123.9, 123.5, 119.6, 115.7, 114.8, 113.0, 110.5. MS-Sciex *m/z* 331.0 [<sup>79</sup>Br, MH<sup>+</sup>], 333.0 [<sup>81</sup>Br, MH<sup>+</sup>]. Anal. (C<sub>14</sub>H<sub>11</sub>BrN<sub>4</sub>O·2.0HCl) C, H, N, Br.

**2-(2-Hydroxy-5-methoxyphenyl)-1H-benzimidazole-5-carboxamide (6g).** Synthesized using general procedure A. <sup>1</sup>H NMR (DMSO-*d*<sub>6</sub>)  $\delta$  9.44 (br s, 2H), 9.13 (br s, 2H), 8.21 (s, 1H), 7.92–7.89 (m, 2H), 7.76 (d, *J* = 8.4 Hz, 1H), 7.09 (s, 2H), 3.80 (s, 3H). <sup>13</sup>C NMR (DMSO-*d*<sub>6</sub>)  $\delta$  165.8, 152.2, 151.5,



137.1, 134.0, 124.1, 123.7, 122.0, 118.4, 115.4, 114.6, 111.5, 109.9, 56.1. MS-Sciex  $m/z$  283.2  $[MH^+]$ . Anal. ( $C_{15}H_{14}N_4O_2 \cdot 1.5HCl \cdot 0.5H_2O$ ) C, H, N.

**2-(2-Hydroxy-3-nitrophenyl)-1H-benzimidazole-5-carboxamide (6h).** Synthesized using general procedure D.  $^1H$  NMR (DMSO- $d_6$ )  $\delta$  9.46 (br s, 2H), 9.19 (br s, 2H), 8.63 (dd,  $J$  = 7.7, 1.3 Hz, 1H), 8.27 (s, 1H), 8.08 (dd,  $J$  = 8.2, 1.3 Hz, 1H), 7.90 (d,  $J$  = 8.6 Hz, 1H), 7.79 (dd,  $J$  = 8.6, 1.7 Hz, 1H), 7.21 (t,  $J$  = 7.9 Hz, 1H).  $^{13}C$  NMR (DMSO- $d_6$ )  $\delta$  166.3, 153.5, 152.9, 139.7, 139.3, 137.2, 132.5, 128.3, 123.9, 123.2, 119.2, 116.9, 115.3. MS-Sciex  $m/z$  298.0  $[MH^+]$ . Anal. ( $C_{14}H_{11}N_5O_3 \cdot 1.5HCl$ ) C, H, N.

**2-(2-Hydroxy-3-methoxyphenyl)-1H-benzimidazole-5-carboxamide (6l).** Synthesized using general procedure A.  $^1H$  NMR (DMSO- $d_6$ )  $\delta$  9.51 (br s, 2H), 9.27 (br s, 2H), 8.22 (s, 1H), 7.90–7.79 (m, 3H), 7.18 (d,  $J$  = 8.2 Hz, 1H), 6.97 (t,  $J$  = 8.2 Hz, 1H), 3.83 (s, 3H).  $^{13}C$  NMR (DMSO- $d_6$ )  $\delta$  166.4, 152.7, 149.1, 148.5, 138.1, 135.2, 124.4, 123.9, 120.1, 116.1, 115.1, 111.4, 56.6. MS-Sciex  $m/z$  283.2  $[MH^+]$ . Anal. ( $C_{15}H_{14}N_4O_2 \cdot 1.5HCl \cdot 0.5H_2O$ ) C, H, N.

**2-(2-Hydroxybiphenyl-3-yl)-1H-benzimidazole-5-carboxamide (6m).** Synthesized using general procedure D.  $^1H$  NMR (DMSO- $d_6$ )  $\delta$  9.39 (br s, 2H), 9.08 (br s, 2H), 8.28–8.13 (m, 2H), 7.85 (d,  $J$  = 8.1 Hz, 1H), 7.74 (d,  $J$  = 8.3 Hz, 1H), 7.65–7.56 (m, 2H), 7.52–7.31 (m, 4H), 7.13 (t,  $J$  = 7.6 Hz, 1H).  $^{13}C$  NMR (DMSO- $d_6$ )  $\delta$  166.0, 155.6, 154.7, 137.5, 133.2, 129.6, 129.2, 128.0, 127.1, 126.3, 122.8, 122.0, 119.3, 112.2. MS-ESI  $m/z$  328.9  $[MH^+]$ . Anal. ( $C_{20}H_{16}N_4O \cdot HCl \cdot 0.5H_2O$ ) C, H, N.

**2-(2-Hydroxy-4-methylphenyl)-1H-benzimidazole-5-carboxamide (6n).** Synthesized using general procedure D.  $^1H$  NMR (DMSO- $d_6$ )  $\delta$  9.56 (br s, 2H), 9.29 (br s, 2H), 8.25–8.22 (m, 2H), 7.95 (d,  $J$  = 8.7 Hz, 1H), 7.84 (d,  $J$  = 8.7 Hz, 1H), 7.09 (s, 1H), 6.93 (d,  $J$  = 8.2 Hz, 1H), 2.35 (s, 3H).  $^{13}C$  NMR (DMSO- $d_6$ )  $\delta$  166.3, 158.5, 152.0, 145.8, 137.3, 134.0, 129.2, 124.7, 124.3, 121.5, 118.0, 115.7, 115.0, 108.0, 21.9. MS-Sciex  $m/z$  266.8  $[MH^+]$ . Anal. ( $C_{15}H_{14}N_4O \cdot 2.0HCl$ ) C, H, N.

**2-(2-Hydroxy-4-diethylaminophenyl)-1H-benzimidazole-5-carboxamide (6o).** Synthesized using general procedure A.  $^1H$  NMR (DMSO- $d_6$ )  $\delta$  9.59 (br s, 2H), 9.32 (br s, 2H), 8.20 (d,  $J$  = 8.4 Hz, 1H), 8.14 (s, 1H), 7.87 (d,  $J$  = 8.4 Hz, 1H), 7.79 (d,  $J$  = 8.8 Hz, 1H), 6.59 (s, 1H), 6.49 (d,  $J$  = 9.1 Hz, 1H), 3.39 (q,  $J$  = 6.6 Hz, 4H), 1.12 (t,  $J$  = 6.6 Hz, 6H).  $^{13}C$  NMR (DMSO- $d_6$ )  $\delta$  165.8, 159.9, 152.8, 149.9, 134.8, 131.1, 130.9, 124.6, 124.1, 113.6, 113.5, 105.4, 97.3, 95.4, 44.4, 12.4. MS-Sciex  $m/z$  324.0  $[MH^+]$ . Anal. ( $C_{18}H_{21}N_5O \cdot 2.0HCl \cdot 0.5H_2O$ ) C, H, N.

**2-(2,6-Dihydroxyphenyl)-1H-benzimidazole-5-carboxamide (6p).** Synthesized using general procedure D.  $^1H$  NMR (DMSO- $d_6$ )  $\delta$  9.54 (br s, 2H), 9.32 (br s, 2H), 8.31 (d,  $J$  = 1.3 Hz, 1H), 8.01 (d,  $J$  = 8.7 Hz, 1H), 7.82 (dd,  $J$  = 8.5, 1.6 Hz, 1H), 7.30 (t,  $J$  = 8.3 Hz, 1H), 6.72 (d,  $J$  = 8.1 Hz, 2H).  $^{13}C$  NMR (DMSO- $d_6$ )  $\delta$  166.1, 158.7, 150.0, 136.1, 134.2, 133.1, 123.8, 123.6, 115.6, 114.7, 107.0, 98.9. MS-Sciex  $m/z$  269.0  $[MH^+]$ . Anal. ( $C_{14}H_{12}N_4O_2 \cdot 2.0HCl$ ) C, H, N.

**2-(1-Hydroxynaphthalen-2-yl)-1H-benzimidazole-5-carboxamide (6q).** Synthesized using general procedure A.  $^1H$  NMR (DMSO- $d_6$ )  $\delta$  9.47 (br s, 2H), 9.22 (br s, 2H), 8.38 (dd,  $J$  = 7.4, 1.5 Hz, 1H), 8.29 (d,  $J$  = 8.6 Hz, 1H), 8.25 (d,  $J$  = 0.9 Hz, 1H), 7.95–7.87 (m, 2H), 7.78 (dd,  $J$  = 8.5, 1.7 Hz, 1H), 7.67–7.55 (m, 3H).  $^{13}C$  NMR (DMSO- $d_6$ )  $\delta$  166.0, 156.0, 154.9, 135.2, 128.5, 127.8, 126.0, 124.6, 123.0, 122.9, 122.2, 119.0, 115.6, 114.5, 105.0. MS-Sciex  $m/z$  303.2  $[MH^+]$ . Anal. ( $C_{18}H_{14}N_4O \cdot 2.0HCl$ ) C, H, N.

**2-(2-Hydroxy-3-bromo-5-methylphenyl)-1H-benzimidazole-5-carboxamide (6r).** Synthesized using general procedure A.  $^1H$  NMR (DMSO- $d_6$ )  $\delta$  9.41 (br s, 2H), 9.13 (br s, 2H), 8.21 (s, 1H), 8.09 (s, 1H), 7.84 (d,  $J$  = 8.4 Hz, 1H), 7.74 (d,  $J$  = 8.4 Hz, 1H), 7.57 (s, 1H), 2.31 (s, 3H).  $^{13}C$  NMR (DMSO- $d_6$ )  $\delta$  165.9, 153.6, 152.7, 139.5, 136.9, 136.0, 129.6, 126.7, 123.1, 122.4, 116.1, 114.6, 112.7, 110.5, 19.8. MS-Sciex  $m/z$  345.0  $[^{79}Br, MH^+]$ , 346.8  $[^{81}Br, MH^+]$ . Anal. ( $C_{15}H_{13}BrN_4O \cdot 1.5HCl$ ) C, H, N.

**2-(2-Hydroxy-5-chlorobiphenyl-3-yl)-1H-benzimidazole-5-carboxamide (6s).** Synthesized using general procedure A.  $^1H$  NMR (DMSO- $d_6$ )  $\delta$  9.47 (br s, 2H), 9.22 (br s, 2H), 8.42 (d,  $J$  = 2.2 Hz, 1H), 8.25 (s, 1H), 7.87 (d,  $J$  = 8.6 Hz, 1H), 7.78 (d,  $J$  = 8.7 Hz, 1H), 7.64 (d,  $J$  = 7.2 Hz, 2H), 7.50–7.36 (m, 4H).  $^{13}C$  NMR (DMSO- $d_6$ )  $\delta$  165.9, 154.5, 153.5, 136.2, 132.3, 131.6, 129.3, 128.2, 127.7, 125.4, 123.1, 122.4, 113.6. MS-Sciex  $m/z$  363.0  $[^{35}Cl, MH^+]$ . Anal. ( $C_{20}H_{15}ClN_4O \cdot 1.5HCl$ ) C, H, N.

**3-Bromo-2-hydroxybenzaldehyde (8).** A solution of 2-bromophenol **7** (6.34 g, 36.6 mmol) in  $CH_3CN$  (170 mL) was treated with  $MgCl_2$  (5.23 g, 55 mmol), paraformaldehyde (7.4 g, 0.25 mol), and finally  $Et_3N$  (12.8 mL, 92 mmol). The mixture was refluxed for 3 h and then allowed to cool. The solution was diluted with 1 N HCl (200 mL) and then extracted with  $Et_2O$  (2  $\times$  200 mL). The organic extracts were washed with brine, dried over  $MgSO_4$ , filtered, and concentrated under reduced pressure to give **8** (6.9 g, 94%) as a yellow oil. This oil was used in subsequent reactions without further purification.  $^1H$  NMR ( $CDCl_3$ )  $\delta$  11.63 (s, 1H), 9.87 (s, 1H), 7.79 (d,  $J$  = 8.1 Hz, 1H), 7.56 (d,  $J$  = 7.5 Hz, 1H), 6.96 (t,  $J$  = 7.8 Hz, 1H).

**2-Hydroxybiphenyl-3-carbaldehyde (10).** Biphenyl-2-ol **9** (17 g, 0.1 mol) was dissolved in THF (200 mL) and then treated with  $Et_3N$  (27 mL, 0.2 mol) followed by  $MgCl_2$  (14.3 g, 0.2 mol). The mixture was stirred for 20 min, and then paraformaldehyde (15 g, 0.5 mol) was added. The resultant mixture was refluxed for 3 h and then diluted with  $EtOAc$  (200 mL). The solution was washed with 1 N HCl followed by brine, dried over  $Na_2SO_4$ , filtered, and concentrated under reduced pressure. The crude product, **10**, (~100%) was sufficiently pure (97% by analytical HPLC) to be used in subsequent reactions. MS-Sciex  $m/z$  199.0  $[MH^+]$ .

**5-Chloro-2-hydroxybiphenyl-3-carbaldehyde (11).** The crude 2-hydroxybiphenyl-3-carbaldehyde **10** (2 g, 10 mmol) was dissolved in AcOH (30 mL) and then treated with *N*-chlorosuccinimide (NCS) (1.5 g, 11 mmol). The mixture was then refluxed for 3 h, allowed to cool, and concentrated under reduced pressure. The residue was dissolved in  $Et_2O$  (100 mL) and the insoluble material removed by filtration. The filtrate was washed with 1 N HCl, followed by brine, dried over  $Na_2SO_4$ , filtered, and concentrated under reduced pressure to give **11** (2.3 g, 98%).  $^1H$  NMR ( $CDCl_3$ )  $\delta$  11.42 (s, 1H), 9.89 (s, 1H), 7.57–7.52 (m, 4H), 7.48–7.38 (m, 3H). MS-Sciex  $m/z$  232.6  $[^{35}Cl, MH^+]$ .

**3-Bromo-2-hydroxy-5-methylbenzaldehyde (13).** A solution of 2-hydroxy-5-methylbenzaldehyde **12** (0.5 g, 3.7 mmol) in AcOH (5 mL) was treated dropwise with bromine (0.21 mL, 4.0 mmol). The resultant mixture was stirred for 1.5 h, and then water was added. The precipitate that formed was collected by filtration and washed with water. The solid was dried to give **13** (0.55 g, 70%).  $^1H$  NMR ( $CDCl_3$ )  $\delta$  11.40 (s, 1H), 9.81 (s, 1H), 7.61 (s, 1H), 7.33 (s, 1H), 2.34 (s, 3H).  $^{13}C$  NMR ( $CDCl_3$ )  $\delta$  195.9, 155.9, 140.6, 132.8, 130.4, 120.9, 110.7, 20.0. MS-Sciex  $m/z$  214.6  $[^{79}Br, MH^+]$ .

**2-(5-Bromo-1H-indol-2-yl)phenol (15).** Prepared according to the procedure of Iwanowicz and co-workers<sup>21</sup> from **14** and **28**.

**2-(2-Hydroxyphenyl)-1H-indole-5-carbonitrile (16).** The 5-bromo-2-phenyl-1H-indole **15** (1.4 g, 4.86 mmol) was dissolved in quinoline (10 mL) and treated with  $CuCN$  (1.31 g, 14.6 mmol). The mixture was heated at 220 °C under nitrogen for 90 min and then cooled. The mixture was treated with  $EtOAc$  (100 mL) and 1 N HCl (100 mL). The organic layer was separated, washed with brine, dried over  $MgSO_4$ , filtered, and concentrated under reduced pressure to give a brown solid. The solid was subjected to chromatography over silica gel eluting with 30%  $EtOAc$  in hexanes to give **16** (0.56 g, 49%).  $^1H$  NMR (DMSO- $d_6$ )  $\delta$  11.70 (s, 1H), 10.30 (s, 1H), 8.04 (s, 1H), 7.75 (d,  $J$  = 7.7 Hz, 1H), 7.60 (d,  $J$  = 8.4 Hz, 1H), 7.39 (dd,  $J$  = 8.4, 1.8 Hz, 1H), 7.19 (m, 1H), 7.09 (s, 1H), 7.01 (d,  $J$  = 8.1 Hz, 1H), 6.92 (t,  $J$  = 7.7 Hz, 1H).

**2-(2-Hydroxyphenyl)-1H-indole-5-carboxamide (19).**<sup>21</sup> The 2-(2-hydroxyphenyl)-1H-indole-5-carbonitrile **16** (0.56 g, 2.4 mmol) was dissolved in absolute EtOH (30 mL), and excess



50% aqueous hydroxylamine (1.0 mL) was added. The mixture was stirred for 18 h at room temperature and then refluxed for 3 h. The mixture was cooled and diluted with EtOAc (150 mL). The organic phase was washed with saturated NaHCO<sub>3</sub> solution, dried over MgSO<sub>4</sub>, filtered, and concentrated under reduced pressure. The crude solid, **17**, was dissolved in AcOH (15 mL) and treated with acetic anhydride (0.25 mL, 2.64 mmol) followed by THF (20 mL). The mixture was stirred for 30 min to give acetate **18** (observed by LCMS), and then 10% Pd/C (50 mg) catalyst was added. The mixture was stirred under hydrogen for 1.5 h. The mixture was then filtered through Celite and the filtrate concentrated under reduced pressure. The crude residue was subjected to preparative HPLC to give **19** (0.24 g, 34%). <sup>1</sup>H NMR (DMSO-*d*<sub>6</sub>) δ 11.73 (s, 1H), 10.39 (s, 1H), 9.16 (s, 2H), 8.84 (s, 2H), 8.10 (s, 1H), 7.79 (d, *J* = 7.7 Hz, 1H), 7.63 (d, *J* = 8.4 Hz, 1H), 7.51 (d, *J* = 8.8 Hz, 1H), 7.19 (t, *J* = 8.0 Hz, 1H), 7.14 (s, 1H), 7.05 (d, *J* = 8.0 Hz, 1H), 6.92 (t, *J* = 8.0 Hz, 1H). <sup>13</sup>C NMR (DMSO-*d*<sub>6</sub>) δ 166.6, 154.7, 139.2, 138.1, 129.0, 127.9, 127.8, 120.9, 120.4, 119.4, 118.1, 117.9, 116.7, 111.8, 101.7. MS-Sciex *m/z* 252.0 [MH<sup>+</sup>]. Anal. (C<sub>15</sub>H<sub>13</sub>N<sub>3</sub>O·HCl·0.25H<sub>2</sub>O) C, H, N, Cl.

**4-Hydrazinobenzamidine (21).** 4-Aminobenzamidine dihydrochloride **20** (10.4 g, 50 mmol) was suspended in 6 N HCl (100 mL) and cooled to 0 °C using an ice bath. A solution of NaNO<sub>2</sub> (3.45 g, 50 mmol) in water (25 mL) was added dropwise with vigorous stirring of the reaction mixture. After the addition was completed, the mixture was stirred for 20 min. Tin(II) chloride dihydrate (22.5 g, 100 mmol) was added in portions and the final mixture stirred for 30 min at 0 °C. The mixture was concentrated under reduced pressure and triturated with absolute EtOH. The decanted solution was concentrated again and triturated with absolute EtOH once more. The residual solid after decantation of the absolute EtOH was collected by filtration and dried. MS-ESI *m/z* 252.0 [MH<sup>+</sup>]. NMR indicated a 60:40 mixture of starting material and product 4-hydrazinobenzamidine dihydrochloride. This was used without further purification although a 2-fold excess of this material had to be used in subsequent reactions.

**General Procedure for the Synthesis of Indoles 22a–k: Example, 2-Hydroxy-5-methylbiphenyl-3-yl)-1H-indole-5-carboxamidines (22e).** 1-(2-Hydroxy-5-methylbiphenyl-3-yl)ethanone **26** (0.32 g, 1.4 mmol) was added to absolute EtOH (10 mL), and 4-hydrazinobenzamidine dihydrochloride **21** (0.66 g, 3.0 mmol) was then added. Triethylamine (1 mL, 7.2 mmol, 5.1 equiv) was added and the resultant solution refluxed for 2 h. The solution was allowed to cool to room temperature and then diluted with Et<sub>2</sub>O (100 mL). The precipitate that formed was collected by filtration and dried to yield the crude hydrazone as the hydrochloride salt (1.66 g). This material typically contains some triethylamine hydrochloride contaminants. The crude hydrazone (1 g) was added to PPA (5 mL) and heated at 140–160 °C for 4.5 h. The reaction was monitored by HPLC for completion. Upon completion the mixture was allowed to cool and then treated with 1 N HCl. The precipitate that formed was collected by filtration and subjected to preparative HPLC to give **22e** (150 mg, 28%) as a brown solid. <sup>1</sup>H NMR (DMSO-*d*<sub>6</sub>) δ 11.95 (s, 1H), 9.26 (br s, 2H), 9.09 (br s, 1H), 8.72 (br s, 1H), 8.18 (s, 1H), 7.66–7.54 (m, 5H), 7.46 (t, *J* = 7.5 Hz, 2H), 7.39–7.33 (m, 1H), 7.13 (s, 1H), 7.06 (d, *J* = 1.5 Hz, 1H), 2.34 (s, 3H). <sup>13</sup>C NMR (DMSO-*d*<sub>6</sub>) δ 166.5, 148.5, 139.2, 138.5, 138.2, 131.9, 131.1, 129.7, 129.3, 128.3, 128.0, 127.8, 127.0, 121.6, 121.0, 120.4, 118.1, 111.7, 102.4, 20.3. MS-Sciex *m/z* 341.8 [MH<sup>+</sup>]. Anal. (C<sub>22</sub>H<sub>19</sub>N<sub>3</sub>O·2.0HCl) C, H, N.

**2-(3-Bromo-2-hydroxy-5-methylphenyl)-1H-indole-5-carboxamidines (22a).** Synthesized using **24** and **21**. <sup>1</sup>H NMR (DMSO-*d*<sub>6</sub>) δ 11.97 (s, 1H), 9.43 (br s, 1H), 9.25 (br s, 2H), 9.06 (br s, 2H), 8.19 (s, 1H), 7.65–7.56 (m, 3H), 7.39 (s, 1H), 7.15 (s, 1H), 2.30 (s, 3H). <sup>13</sup>C NMR (DMSO-*d*<sub>6</sub>) δ 166.5, 148.4, 139.2, 137.0, 132.5, 131.0, 128.1, 127.7, 122.0, 121.2, 120.8, 118.3, 113.3, 111.7, 103.1, 19.8. MS-Sciex *m/z* 344.0 [<sup>79</sup>Br, MH<sup>+</sup>]. Anal. (C<sub>16</sub>H<sub>14</sub>BrN<sub>3</sub>O·HCl) C, H, N.

**2-(3-Bromo-2-hydroxyphenyl)-1H-indole-5-carboxamidines (22b).** Synthesized using **29** and **21**. <sup>1</sup>H NMR (DMSO-

*d*<sub>6</sub>) δ 11.86 (s, 1H), 9.65 (br s, 1H), 9.11 (br s, 2H), 8.96 (br s, 2H), 8.11 (s, 1H), 7.71 (dd, *J* = 7.7, 1.5 Hz, 1H), 7.52 (m, 3H), 7.09 (s, 1H), 6.91 (t, *J* = 7.9 Hz, 1H). <sup>13</sup>C NMR (DMSO-*d*<sub>6</sub>) δ 166.4, 150.7, 139.2, 136.9, 132.4, 127.8, 127.7, 122.3, 121.8, 121.3, 120.8, 118.4, 113.3, 111.8, 103.1. MS-Sciex *m/z* 329.4 [<sup>79</sup>Br, M<sup>+</sup>], 331.2 [<sup>81</sup>Br, M<sup>+</sup>]. Anal. (C<sub>15</sub>H<sub>12</sub>BrN<sub>3</sub>O·C<sub>2</sub>H<sub>5</sub>F<sub>3</sub>O<sub>2</sub>) Calcd: C, 45.97; H, 2.95; N, 9.46; Br, 17.99. Found: C, 46.08; H, 2.97; N, 9.94; Br, 17.88.

**2-(3,5-Dibromo-2-hydroxyphenyl)-1H-indole-5-carboxamidines (22c).** Synthesized using a commercially available 1-(3,5-dibromo-2-hydroxyphenyl)ethanone and **21**. <sup>1</sup>H NMR (DMSO-*d*<sub>6</sub>) δ 12.00 (s, 1H), 10.03 (br s, 1H), 9.19 (br s, 2H), 8.84 (br s, 2H), 8.17 (s, 1H), 7.97 (d, *J* = 2.4 Hz, 1H), 7.78 (d, *J* = 2.3 Hz, 1H), 7.63–7.56 (m, 2H), 7.26 (s, 1H). <sup>13</sup>C NMR (DMSO-*d*<sub>6</sub>) δ 167.0, 150.9, 139.9, 135.8, 134.1, 130.2, 128.1, 124.5, 122.2, 121.8, 119.1, 115.0, 112.7, 112.4, 104.9. MS-Sciex *m/z* 407.6 [2 × <sup>79</sup>Br, MH<sup>+</sup>]. Anal. (C<sub>15</sub>H<sub>11</sub>Br<sub>2</sub>N<sub>3</sub>O·HCl·0.5H<sub>2</sub>O) C, H, N, Cl.

**2-(3-Bromo-2-hydroxy-5-nitrophenyl)-1H-indole-5-carboxamidines (22d).** Synthesized using **31** and **21**. <sup>1</sup>H NMR (DMSO-*d*<sub>6</sub>) δ 12.32 (s, 1H), 9.20 (br s, 2H), 8.85 (br s, 2H), 8.64 (d, *J* = 2.7 Hz, 1H), 8.40 (d, *J* = 2.7 Hz, 1H), 8.19 (s, 1H), 7.65 (d, *J* = 8.4 Hz, 1H), 7.59 (d, *J* = 8.4 Hz, 1H), 7.31 (s, 1H). <sup>13</sup>C NMR (DMSO-*d*<sub>6</sub>) δ 166.4, 158.2, 139.6, 139.3, 135.1, 127.6, 127.3, 122.7, 121.7, 121.4, 121.3, 118.7, 112.8, 111.9, 104.4. MS-Sciex *m/z* 374.6 [<sup>79</sup>Br, MH<sup>+</sup>], 376.6 [<sup>81</sup>Br, MH<sup>+</sup>]. Anal. (C<sub>15</sub>H<sub>11</sub>BrN<sub>4</sub>O<sub>3</sub>·HCl·0.5H<sub>2</sub>O) C, H, N.

**2-(2-Hydroxybiphenyl-3-yl)-1H-indole-5-carboxamidines (22f).** Synthesized using **35** and **21**. <sup>1</sup>H NMR (DMSO-*d*<sub>6</sub>) δ 11.96 (s, 1H), 9.24 (br s, 2H), 9.02 (br s, 1H), 8.97 (s, 1H), 8.18 (s, 1H), 7.76 (dd, *J* = 7.7, 1.7 Hz, 1H), 7.65 (d, *J* = 8.7 Hz, 1H), 7.59 (dd, *J* = 3.0, 1.7 Hz, 1H), 7.55 (m, 2H), 7.48 (t, *J* = 7.6 Hz, 2H), 7.41–7.35 (m, 1H), 7.25 (dd, *J* = 7.5, 1.7 Hz, 1H), 7.14 (s, 1H), 7.11 (t, *J* = 7.7 Hz, 1H). <sup>13</sup>C NMR (DMSO-*d*<sub>6</sub>) δ 166.5, 150.8, 139.2, 138.3, 138.0, 131.9, 130.5, 129.3, 128.4, 127.8, 127.1, 121.7, 121.0, 120.5, 118.1 (× 2), 111.7, 102.5. MS-Sciex *m/z* 328.2 [MH<sup>+</sup>]. Anal. (C<sub>21</sub>H<sub>17</sub>N<sub>3</sub>O·HCl) C, H, N, Cl.

**2-(5-Bromo-2-hydroxybiphenyl-3-yl)-1H-indole-5-carboxamidines (22g).** Synthesized using **37** and **21**. <sup>1</sup>H NMR (DMSO-*d*<sub>6</sub>) δ 11.98 (s, 1H), 9.18 (br s, 2H), 9.14 (br s, 2H), 8.18 (s, 1H), 7.94 (d, *J* = 2.5 Hz, 1H), 7.66–7.37 (m, 8H), 7.25 (d, *J* = 1.0 Hz, 1H). <sup>13</sup>C NMR (DMSO-*d*<sub>6</sub>) δ 167.0, 159.6, 159.1, 151.0, 139.8, 137.5, 136.8, 134.6, 132.7, 129.9, 129.0, 128.3, 124.5, 121.9, 121.5, 119.1, 113.0, 112.4, 104.2. MS-Sciex *m/z* 405.8 [<sup>79</sup>Br, MH<sup>+</sup>]. Anal. (C<sub>21</sub>H<sub>16</sub>BrN<sub>3</sub>O·C<sub>2</sub>H<sub>5</sub>F<sub>3</sub>O<sub>2</sub>) C, H, N, Br.

**2-(5-Chloro-2-hydroxybiphenyl-3-yl)-1H-indole-5-carboxamidines (22h).** Synthesized using **36** and **21**. <sup>1</sup>H NMR (DMSO-*d*<sub>6</sub>) δ 11.96 (s, 1H), 9.19 (br s, 1H), 9.17 (br s, 1H), 8.92 (br s, 2H), 8.12 (s, 1H), 7.77 (d, *J* = 2.5 Hz, 1H), 7.56–7.34 (m, 7H), 7.20 (d, *J* = 2.5 Hz, 1H), 7.18 (s, 1H). <sup>13</sup>C NMR (DMSO-*d*<sub>6</sub>) δ 166.3, 149.8, 139.2, 137.0, 136.4, 133.7, 129.3, 128.8, 128.5, 127.7, 126.5, 124.7, 123.5, 121.4, 120.9, 118.3 (× 2), 111.8, 103.6. MS-Sciex *m/z* 362.0 [<sup>35</sup>Cl, MH<sup>+</sup>]. Anal. (C<sub>21</sub>H<sub>16</sub>ClN<sub>3</sub>O·HCl·0.5H<sub>2</sub>O) C, H, N.

**2-(5-Nitro-2-hydroxybiphenyl-3-yl)-1H-indole-5-carboxamidines (22i).** Synthesized using **32** and **21**. <sup>1</sup>H NMR (DMSO-*d*<sub>6</sub>) δ 12.25 (br s, 1H), 9.19 (br s, 2H), 8.80 (br s, 2H), 8.64 (d, *J* = 3.0 Hz, 1H), 8.19 (s, 1H), 8.03 (d, *J* = 2.7 Hz, 1H), 7.68–7.44 (m, 7H), 7.31 (s, 1H). <sup>13</sup>C NMR (DMSO-*d*<sub>6</sub>) δ 166.4, 157.9, 140.4, 139.3, 136.4, 135.6, 131.7, 129.3, 128.7, 128.1, 127.7, 125.2, 122.8, 121.8, 121.6, 121.2, 118.6, 111.9, 104.2. MS-Sciex *m/z* 373.0 [MH<sup>+</sup>]. Anal. (C<sub>21</sub>H<sub>16</sub>N<sub>4</sub>O<sub>3</sub>·HCl·H<sub>2</sub>O) C, H, N.

**2-Biphenyl-3-yl-1H-indole-5-carboxamidines (22j).** Synthesized using **27** and **21**. <sup>1</sup>H NMR (DMSO-*d*<sub>6</sub>) δ 9.30 (br s, 2H), 9.11 (br s, 2H), 8.29 (s, 1H), 8.19 (s, 1H), 7.97 (d, *J* = 7.7 Hz, 1H), 7.83 (d, *J* = 7.4 Hz, 2H), 7.68–7.57 (m, 4H), 7.51 (t, *J* = 7.6 Hz, 2H), 7.41 (t, *J* = 7.4 Hz, 1H), 7.24 (d, *J* = 1.7 Hz, 1H). <sup>13</sup>C NMR (DMSO-*d*<sub>6</sub>) δ 167.1, 141.5, 140.8, 140.6, 140.3, 132.5, 130.2, 129.5, 128.7, 128.3, 127.5, 126.9, 125.2, 124.1, 121.9, 121.6, 119.2, 112.3, 100.6. MS-Sciex *m/z* 311.6 [MH<sup>+</sup>]. Anal. (C<sub>21</sub>H<sub>17</sub>N<sub>3</sub>·HCl·0.5H<sub>2</sub>O) C, H, N.

**2-(2-Methoxybiphenyl-3-yl)-1*H*-indole-5-carboxamide (22k).** Synthesized using **39** and **21**. <sup>1</sup>H NMR (DMSO-*d*<sub>6</sub>) δ 12.08 (s, 1H), 9.26 (br s, 2H), 9.09 (br s, 1H), 8.20 (s, 1H), 7.90 (dd, *J* = 6.7, 2.5 Hz, 1H), 7.69–7.59 (m, 4H), 7.49 (t, *J* = 7.0 Hz, 2H), 7.44–7.34 (m, 3H), 7.17 (s, 1H), 3.27 (s, 3H). <sup>13</sup>C NMR (DMSO-*d*<sub>6</sub>) δ 166.5, 154.5, 139.5, 137.7, 136.8, 135.8, 130.9, 128.9, 128.4, 128.1, 127.8, 127.5, 125.2, 124.8, 121.3, 120.9, 118.4, 111.9, 102.8, 59.9. MS-Sciex *m/z* 341.4 [*M*<sup>+</sup>]. Anal. (C<sub>22</sub>H<sub>19</sub>N<sub>3</sub>O·HCl·0.25H<sub>2</sub>O) C, H, N.

**1-(3-Bromo-2-hydroxy-5-methylphenyl)ethanone (24).** 1-(2-Hydroxy-5-methylphenyl)ethanone **23** (10.0 g, 66.6 mmol) was dissolved in MeOH (200 mL) and treated with *N*-bromosuccinimide (NBS) (11.85 g, 66.6 mmol). The mixture was stirred for 3 h and then water (100 mL) was added. The resultant pale yellow solid that formed was collected by filtration and washed with water. The solid was dried to give **24** (13 g, 85%). <sup>1</sup>H NMR (DMSO-*d*<sub>6</sub>) δ 7.57 (d, *J* = 2.2 Hz, 1H), 7.48 (dd, *J* = 2.0, 0.7 Hz, 1H), 2.63 (s, 3H), 2.30 (s, 3H). MS-Sciex *m/z* 229.0 [<sup>79</sup>Br, *M*-H<sup>+</sup>], 231.0 [<sup>81</sup>Br, *M*-H<sup>+</sup>].

**1-(2-Hydroxy-5-methylbiphenyl-3-yl)ethanone (26).** 1-(3-Bromo-2-hydroxy-5-methylphenyl)ethanone **24** (0.46 g, 2 mmol) and phenylboronic acid (0.24 g, 2 mmol) were dissolved in ethylene glycol dimethyl ether (DME) (10 mL). NaHCO<sub>3</sub> (0.50 g, 6 mmol) in water (10 mL) was added followed by tetrakis(triphenylphosphine)palladium(0) (0.12 g, 0.1 mmol). The reaction mixture was refluxed for 10 min and then heated at 75 °C overnight. Most of the DME was then removed under reduced pressure. The resultant mixture was diluted with Et<sub>2</sub>O (100 mL), washed with water and brine, and then dried over MgSO<sub>4</sub>. The organic solution was filtered and concentrated under reduced pressure. The crude solid was subjected to chromatography over silica gel eluting with 10% EtOAc in hexanes to give **26** (0.32 g, 71% yield) as a yellow solid. <sup>1</sup>H NMR (DMSO-*d*<sub>6</sub>) δ 7.58–7.52 (m, 3H), 7.45–7.31 (m, 4H), 2.66 (s, 3H), 2.35 (s, 3H). MS-Sciex *m/z* 224.8 [*M*-H<sup>+</sup>].

**1-Biphenyl-3-yl-ethanone (27).** 1-(3-Bromophenyl)ethanone **25** (2.0 g, 10 mmol) was mixed with phenylboronic acid (1.2 g, 10 mmol) in THF (100 mL). Tetrakis(triphenylphosphine)palladium(0) (1.1 g, 1 mmol) was added followed by K<sub>2</sub>CO<sub>3</sub> (4.1 g, 30 mmol) and the resultant mixture refluxed overnight. The mixture was allowed to cool and then filtered through Celite. The eluant was diluted with EtOAc (500 mL) and washed with saturated NaHCO<sub>3</sub> solution (2 × 300 mL) followed by brine. The organic solution was dried over Na<sub>2</sub>SO<sub>4</sub>, filtered, and concentrated under reduced pressure. The residue was subjected to chromatography over silica gel eluting with 10% EtOAc in hexanes to give **27** (1.2 g, 61%). <sup>1</sup>H NMR (CDCl<sub>3</sub>) δ 8.18 (t, *J* = 2.0 Hz, 1H), 7.98–7.91 (m, 2H), 7.76–7.72 (m, 2H), 7.62 (t, *J* = 7.9 Hz, 1H), 7.54–7.39 (m, 3H), 2.66 (s, 3H).

**1-(3-Bromo-2-hydroxyphenyl)ethanone (29).** 1-(2-Hydroxyphenyl)ethanone **28** (1.36 g, 10 mmol) was dissolved in AcOH (20 mL) and treated with NBS (1.78 g, 10 mmol). The mixture was stirred overnight and then concentrated under reduced pressure. The residual solid was dissolved in Et<sub>2</sub>O (100 mL) and washed with brine. The organic solution was dried over Na<sub>2</sub>SO<sub>4</sub>, filtered, and concentrated under reduced pressure. The residue was subjected to chromatography over silica gel eluting with 5% EtOAc in hexanes to give **29** (198 mg, 9%). <sup>1</sup>H NMR (CDCl<sub>3</sub>) δ 7.74 (dd, *J* = 7.9, 2.2 Hz, 1H), 7.72 (dd, *J* = 7.9, 1.5 Hz, 1H), 6.81 (t, *J* = 7.9 Hz, 1H), 2.65 (s, 3H).

**1-(2-Hydroxy-5-nitrophenyl)ethanone (30).** 1-(2-Hydroxyphenyl)ethanone **28** (13.6 g, 0.1 mol) was dissolved in AcOH (100 mL) and cooled to 0 °C using an ice bath. Fuming HNO<sub>3</sub> (6.3 mL, 0.15 mol) was added over 30 min, and the solution was stirred overnight at room temperature. The solution was concentrated under reduced pressure and the residual oil treated with water to yield a solid. The solid was collected and redissolved in Et<sub>2</sub>O (200 mL). The organic solution was washed with water (5 × 100 mL) and then brine. The organic layer was dried over Na<sub>2</sub>SO<sub>4</sub>, filtered, and concentrated under reduced pressure to yield the crude product. The crude product was subjected to chromatography over silica gel eluting with 10% EtOAc in hexanes to give **30** (6.5 g, 36%). <sup>1</sup>H NMR (CDCl<sub>3</sub>)

δ 8.70 (d, *J* = 2.7 Hz, 1H), 8.34 (ddd, *J* = 9.1, 2.7, 0.5 Hz, 1H), 7.08 (d, *J* = 9.1 Hz, 1H), 2.73 (s, 3H). MS-Sciex *m/z* 179.6 [*M*-H<sup>+</sup>].

**1-(3-Bromo-2-hydroxy-5-nitrophenyl)ethanone (31).** The acetophenone **30** (1.8 g, 10 mmol) was dissolved in CH<sub>3</sub>CN (50 mL) and treated with NBS (1.78 g, 10 mmol). The resultant solution was stirred overnight and then diluted with EtOAc (250 mL). The organic solution was washed with brine (2 × 200 mL), water (2 × 200 mL), and brine (2 × 200 mL) again. The organic solution was then dried over Na<sub>2</sub>SO<sub>4</sub>, filtered, and concentrated under reduced pressure. The residue was dissolved in hot MeOH and then treated with water. The solid precipitate that formed was collected by filtration and dried to give **31** (1.46 g, 56%). <sup>1</sup>H NMR (CDCl<sub>3</sub>) δ 8.74 (d, *J* = 2.7 Hz, 1H), 8.68 (d, *J* = 2.7 Hz, 1H), 2.79 (s, 3H). MS-Sciex *m/z* 257.8 [<sup>79</sup>Br, *M*-H<sup>+</sup>], 259.4 [<sup>81</sup>Br, *M*-H<sup>+</sup>].

**1-(2-Hydroxy-5-nitrobiphenyl-3-yl)ethanone (32).** The nitroarene **31** (464 mg, 1.8 mmol) was mixed with phenylboronic acid (272 mg, 2.2 mmol) in THF (15 mL). The mixture was then treated with tetrakis(triphenylphosphine)palladium(0) (103 mg, 0.089 mmol) and 10% Na<sub>2</sub>CO<sub>3</sub> solution (2 mL). The mixture was heated at 80 °C for 2 h and then a further portion of tetrakis(triphenylphosphine)palladium(0) (103 mg, 0.089 mmol) was added. After the mixture was heated for another 1 h, 10% Pd/C catalyst (150 mg) was added and heating continued for 1.5 h. The mixture was allowed to cool, diluted with EtOAc (60 mL), and then filtered through Celite. The eluant was washed with brine, 1 N HCl, and finally brine again. The organic solution was then dried over Na<sub>2</sub>SO<sub>4</sub>, filtered, and concentrated under reduced pressure. The crude product was subjected to chromatography over silica gel eluting with 50% EtOAc in hexanes to give **32** (322 mg, 70%). <sup>1</sup>H NMR (CDCl<sub>3</sub>) δ 8.70 (d, *J* = 2.7 Hz, 1H), 8.43 (dd, *J* = 2.7, 0.7 Hz, 1H), 7.60–7.55 (m, 2H), 7.50–7.41 (m, 3H), 2.79 (s, 3H). <sup>13</sup>C NMR (CDCl<sub>3</sub>) δ 204.4, 164.7, 139.2, 134.6, 132.5, 131.1, 129.2, 128.5, 128.4, 125.8, 118.6, 26.9.

**2-Hydroxybiphenyl-3-carboxylic Acid *N*-Methoxy-*N*-methylamide (34).** 2-Hydroxy-3-phenylbenzoic acid **33** (5.35 g, 25 mmol) was dissolved in dry DMF (50 mL) and cooled to 0 °C. PyBOP (13.65 g, 26.3 mmol) was added followed by *N*,*O*-dimethylhydroxylamine hydrochloride (2.56 g, 26.8 mmol) and finally *N*,*N*-diisopropylethylamine (DIEA) (11 mL, 63 mmol). The mixture was stirred for 3 h and allowed to warm to room temperature. The solvent was removed under reduced pressure and the residue dissolved in 20% 2-propanol in CH<sub>2</sub>Cl<sub>2</sub>. The solution was washed with saturated NaHCO<sub>3</sub>, dried over MgSO<sub>4</sub>, filtered, and concentrated under reduced pressure to give a golden oil. The oil was subjected to chromatography over silica gel eluting with 20% EtOAc in hexanes to give **34** (4.5 g, 71%) as a white solid. <sup>1</sup>H NMR (CDCl<sub>3</sub>) δ 11.42 (s, 1H), 7.94 (dd, *J* = 8.1, 1.7 Hz, 1H), 7.61–7.58 (m, 1H), 7.48–7.36 (m, 6H), 6.93 (t, *J* = 2.9 Hz, 1H), 3.70 (s, 3H), 3.45 (s, 3H).

**1-(2-Hydroxybiphenyl-3-yl)ethanone (35).** 2-Hydroxybiphenyl-3-carboxylic acid *N*-methoxy-*N*-methylamide **34** (1.96 g, 7.6 mmol) was dissolved in dry Et<sub>2</sub>O (40 mL) and cooled to 0 °C. A 1.4 M solution of MeLi in Et<sub>2</sub>O (16.3 mL, 22.8 mmol) was added dropwise, and the heterogeneous reaction mixture was then stirred for 1 h. The reaction mixture was quenched with dilute 1 N HCl. The organic layer was separated, washed with brine, dried over MgSO<sub>4</sub>, filtered, and concentrated under reduced pressure. The crude product was subjected to chromatography over silica gel eluting with 5% EtOAc in hexanes to give **35** (1.07 g, 66%) as a white solid. <sup>1</sup>H NMR (CDCl<sub>3</sub>) δ 7.75 (dd, *J* = 8.0, 1.8 Hz, 1H), 7.59–7.53 (m, 3H), 7.46–7.34 (m, 3H), 6.97 (t, *J* = 7.7 Hz, 1H), 2.68 (s, 3H).

**1-(5-Chloro-2-hydroxybiphenyl-3-yl)ethanone (36).** 1-(2-Hydroxybiphenyl-3-yl)ethanone **35** (1.03 g, 4.9 mmol) was dissolved in DMF (20 mL) and then treated with NCS (1.3 g, 9.7 mmol). The mixture was stirred overnight and then concentrated under reduced pressure. The residue was dissolved in Et<sub>2</sub>O (100 mL) and washed with water, Na<sub>2</sub>S<sub>2</sub>O<sub>3</sub> solution, and finally brine. The organic solution was then dried over Na<sub>2</sub>SO<sub>4</sub>, filtered, and concentrated under reduced pres-



sure to give the crude **36** (1.16 g, 96%) which could be used without further purification.

**1-(5-Bromo-2-hydroxybiphenyl-3-yl)ethanone (37).** 1-(2-Hydroxybiphenyl-3-yl)ethanone **35** (0.85 g, 4 mmol) was dissolved in AcOH (5 mL) and then treated with NBS (0.71 g, 4 mmol). The mixture was heated at 85 °C for 2 h. The mixture was concentrated under reduced pressure and the resultant solid dissolved in Et<sub>2</sub>O (50 mL). The organic solution was washed with water followed by brine. The organic layer was dried over Na<sub>2</sub>SO<sub>4</sub>, filtered, and concentrated under reduced pressure to give **37** (1.16 g, ~100%). <sup>1</sup>H NMR (CDCl<sub>3</sub>) δ 7.84 (d, *J* = 2.5 Hz, 1H), 7.64 (d, *J* = 2.5 Hz, 1H), 7.55–7.52 (m, 2H), 7.46–7.36 (m, 3H), 2.66 (s, 3H).

**2-Methoxybiphenyl-3-carbaldehyde (38).** 2-Hydroxybiphenyl-3-carbaldehyde **10** (2.0 g, 10 mmol) in DMF (30 mL) was treated with cesium carbonate (3.9 g, 12 mmol) and MeI (0.69 mL, 11 mmol). The mixture was stirred overnight and then diluted with EtOAc (200 mL). The solution was washed with Na<sub>2</sub>S<sub>2</sub>O<sub>5</sub> solution and then brine. The organic solution was dried over Na<sub>2</sub>SO<sub>4</sub>, filtered, and concentrated under reduced pressure. The residual solid was subjected to chromatography over silica gel eluting with 5% EtOAc in hexanes to give **38** (1.2 g, 56%). <sup>1</sup>H NMR (CDCl<sub>3</sub>) δ 10.47 (s, 1H), 7.84 (dd, *J* = 7.7, 1.8 Hz, 1H), 7.61–7.55 (m, 3H), 7.48–7.38 (m, 3H), 7.29 (dd, *J* = 7.6, 1.0 Hz, 1H), 3.50 (s, 3H).

**1-(2-Methoxybiphenyl-3-yl)ethanone. (39).** Vanadium(III) chloride (0.89 g, 5.65 mmol) was added to CH<sub>2</sub>Cl<sub>2</sub> (10 mL) and cooled to –78 °C. A 3 M solution of MeMgBr in Et<sub>2</sub>O (1.9 mL, 5.65 mmol) was added in two portions over 10 min, and the resultant mixture was then stirred for 20 min. This solution was then added to a solution of the aldehyde **38** (1.2 g, 5.65 mmol) in CH<sub>2</sub>Cl<sub>2</sub> (10 mL) at –78 °C. After stirring the mixture for 2 h at –78 °C, the solution was allowed to warm to room temperature. Toluene (20 mL) was added and the solution refluxed overnight. The solution was allowed to cool and then diluted with EtOAc (200 mL) and washed with saturated NaHCO<sub>3</sub> (2 × 100 mL), water (2 × 100 mL), and finally brine. The organic solution was dried over Na<sub>2</sub>SO<sub>4</sub>, filtered, and concentrated under reduced pressure. The residual solid was subjected to chromatography over silica gel eluting with 15% EtOAc in hexanes to give the intermediate alcohol. The alcohol was then dissolved in dry CH<sub>2</sub>Cl<sub>2</sub> and treated with 4-methylmorpholine-*N*-oxide (0.79 g, 6.75 mmol) followed by tetrapropylammonium perruthenate (TPAP). The mixture was stirred for 60 min and then filtered through silica gel eluting with CH<sub>2</sub>Cl<sub>2</sub>. The eluant was concentrated under reduced pressure to give **39** (0.9 g, 70%). <sup>1</sup>H NMR (CDCl<sub>3</sub>) δ 7.60 (dd, *J* = 7.7, 1.7 Hz, 1H), 7.57–7.53 (m, 2H), 7.48–7.36 (m, 4H), 7.21 (t, *J* = 7.7 Hz, 1H), 3.40 (s, 3H), 2.67 (s, 3H).

**3-Methoxy-4-nitrobenzonitrile (43).** The 3-methoxy-4-nitrobenzoic acid **40** (5.2 g, 26.4 mmol) was dissolved in THF (70 mL) and cooled to 0 °C with an ice bath. Oxalyl chloride (2.53 mL, 29.0 mmol) was added followed by several drops of DMF. The ice bath was removed and the solution stirred for 1 h. The mixture was concentrated under reduced pressure to give **41** as a yellow solid. Crude solid **41** was dissolved in THF (70 mL) and cooled to 0 °C with an ice bath. Ammonia gas was bubbled through the solution for 10 min, which resulted in the formation of a pale yellow slurry. The ice bath was removed and the addition of ammonia gas continued for a further 5 min. The mixture was then sealed, stirred overnight, and then diluted with EtOAc (600 mL). The organic mixture was washed with 1 N HCl, brine, dried over MgSO<sub>4</sub>, filtered, and concentrated under reduced pressure to give **42** (3.65 g, 71%) as a yellow solid. <sup>1</sup>H NMR (DMSO-*d*<sub>6</sub>) δ 8.23 (br s, 1H), 7.94 (d, *J* = 8.4 Hz, 1H), 7.72 (d, *J* = 1.5 Hz, 1H), 7.71 (br s, 1H), 7.56 (dd, *J* = 8.4, 1.5 Hz, 1H), 3.97 (s, 3H). The crude solid **42** (3.6 g, 18.4 mmol) was stirred in THF (50 mL), and Et<sub>3</sub>N (3.3 mL, 23.9 mmol) was added. The yellow slurry was then treated with TFA (2.85 mL, 20.2 mmol) by slow addition. After 1 h the solution was concentrated under reduced pressure and diluted with EtOAc (300 mL). The solution was washed with 1 N HCl (200 mL), saturated NaHCO<sub>3</sub> solution (2 × 200 mL), and then brine. The organic solution was dried

over Na<sub>2</sub>SO<sub>4</sub>, filtered, and concentrated under reduced pressure to give **43** (3.26 g, ~100% from **40**) as a yellow solid. <sup>1</sup>H NMR (DMSO-*d*<sub>6</sub>) δ 8.04 (d, *J* = 8.1 Hz, 1H), 7.94 (s, 1H), 7.60 (d, *J* = 8.1 Hz, 1H), 3.96 (s, 3H).

**3-Methylamino-4-nitrobenzonitrile (44).** The crude 3-methoxy-4-nitrobenzonitrile **43** (1.0 g, 5.6 mmol) was stirred in DMSO (7 mL) and heated to 75 °C. A 40% solution of methylamine in water (1 mL) was added and the mixture heated at 75 °C for 2 h. The solution was allowed to cool, and then EtOAc (200 mL) was added. The solution was washed with 10% NaHCO<sub>3</sub> (3 × 100 mL) followed by brine. The organic solution was dried over Na<sub>2</sub>SO<sub>4</sub>, filtered, and concentrated under reduced pressure to give **44** (0.91 g, 92%) as an orange solid. <sup>1</sup>H NMR (DMSO-*d*<sub>6</sub>) δ 8.24 (br q, *J* = 5.1 Hz, 1H), 8.17 (d, *J* = 8.8 Hz, 1H), 7.51 (s, 1H), 7.00 (d, *J* = 8.8 Hz, 1H), 2.96 (d, *J* = 5.1 Hz, 3H).

**4-Amino-3-methylaminobenzonitrile (45).** 3-Methylamino-4-nitrobenzonitrile **44** (0.85 g, 4.8 mmol) was dissolved in MeOH (50 mL) and EtOAc (50 mL). 10% Pd/C (200 mg) catalyst was added and the mixture stirred under hydrogen at atmospheric pressure for 1.5 h. The mixture was filtered through Celite and the eluant concentrated under reduced pressure to give **45** (0.69 g, ~98%) as a tan solid. <sup>1</sup>H NMR (DMSO-*d*<sub>6</sub>) δ 6.84 (dd, *J* = 7.7, 1.4 Hz, 1H), 6.56 (m, 2H), 5.45 (br s, 2H), 4.98 (br s, 1H), 2.71 (s, 3H).

**2-(2-Hydroxybiphenyl-3-yl)-3-methyl-3H-benzimidazole-5-carbonitrile (46).** The 4-amino-3-methylaminobenzonitrile **45** (0.64 g, 4.35 mmol) and 2-hydroxybiphenyl-3-carbaldehyde **10** (1.03 g, 5.22 mmol) were reacted according to general procedure C. The crude product was subjected to chromatography over silica gel eluting with 25% EtOAc in hexanes to give **46** (1.22 g, 86%). <sup>1</sup>H NMR (DMSO-*d*<sub>6</sub>) δ 8.39 (s, 1H), 7.86 (m, 2H), 7.69 (dd, *J* = 8.0, 1.1 Hz, 1H), 7.60 (m, 2H), 7.56–7.35 (m, 4H), 7.14 (m, 1H), 4.03 (s, 3H).

**2-(2-Hydroxyphenyl)-3-methyl-3H-benzimidazole-5-carboxamide (49).** The 2-(2-hydroxybiphenyl-3-yl)-3-methyl-3H-benzimidazole-5-carbonitrile **46** (1.22 g, 3.8 mmol) was dissolved in DMSO (15 mL) and heated to 70 °C. A 50% aqueous solution of hydroxylamine (2 mL) was added and the mixture heated at 70 °C for 1 h. The mixture was cooled, diluted with water (200 mL), and the resultant precipitate that formed was collected by filtration to give the crude hydroxylamide product **47** (1.07 g, 80%). <sup>1</sup>H NMR (DMSO-*d*<sub>6</sub>) δ 8.50 (s, 1H), 7.98 (d, *J* = 8.5 Hz, 1H), 7.82 (d, *J* = 8.5 Hz, 1H), 7.75 (d, *J* = 8.1 Hz, 1H), 7.60–7.57 (m, 3H), 7.47–7.35 (m, 3H), 7.20 (t, *J* = 7.7 Hz, 1H), 4.00 (s, 3H). A portion of **47** (0.3 g, 0.84 mmol) was dissolved in AcOH (30 mL) and then treated with acetic anhydride (80 μL, 0.88 mmol). After the solution was stirred for 50 min, 10% Pd/C (50 mg) catalyst was added. The mixture was stirred under hydrogen at atmospheric pressure for 2 h and then filtered through Celite. The eluant was concentrated under reduced pressure and the crude residue subjected to preparative HPLC to give **49** (0.12 g, 42% from **47**) as a tan solid. <sup>1</sup>H NMR (DMSO-*d*<sub>6</sub>) δ 9.70 (br s, 2H), 9.41 (br s, 2H), 8.69 (s, 1H), 8.01 (m, 2H), 7.76 (d, *J* = 7.7 Hz, 1H), 7.60 (m, 3H), 7.49–7.38 (m, 3H), 7.23 (m, 1H), 4.04 (s, 3H). <sup>13</sup>C NMR (DMSO-*d*<sub>6</sub>) δ 165.1, 153.4, 152.4, 137.3, 136.6, 135.0, 133.4, 131.5, 130.6, 129.4, 128.3, 127.4, 124.9, 123.9, 120.6, 115.7, 114.2, 112.7, 33.0. MS-Sciex *m/z* = 342.8 [MH<sup>+</sup>]. Anal. (C<sub>21</sub>H<sub>18</sub>N<sub>4</sub>O·2.0HCl) C, H, N, Cl.

**4-Hydroxy-3-iodobenzonitrile (51).** The 4-hydroxybenzonitrile **50** (2.4 g, 20 mmol) was dissolved in AcOH (40 mL) and treated with *N*-iodosuccinimide (NIS) (4.5 g, 20 mmol). The mixture was stirred overnight and the precipitate removed by filtration. The filtrate was concentrated under reduced pressure and the resultant oil dissolved in Et<sub>2</sub>O. The insoluble material was removed by filtration and the filtrate washed with saturated NaHCO<sub>3</sub>. The organic phase was dried over MgSO<sub>4</sub>, filtered, and concentrated under reduced pressure. The crude residue was subjected to chromatography over silica gel eluting with 10% MeOH in CH<sub>2</sub>Cl<sub>2</sub> to give **51** (2.0 g, 40%) (90% pure by analytical HPLC). <sup>1</sup>H NMR (CDCl<sub>3</sub>) δ 7.96 (d, *J* = 2.0 Hz, 1H), 7.54 (dd, *J* = 8.7, 2.0 Hz, 1H), 7.04 (d, *J* = 8.7 Hz, 1H), 5.92 (s, 1H).



**2-(2-Methoxyethoxymethoxy)biphenyl-3-carbaldehyde (52).** The 2-hydroxy-3-phenylbenzaldehyde **10** (1.7 g, 8.6 mmol) was dissolved in DMF (20 mL) and then treated with DIEA (1.8 mL, 10.1 mmol) followed by 2-methoxyethoxymethyl chloride (1.2 mL, 10.1 mmol). After 2 h the mixture was diluted with EtOAc (350 mL) and water (200 mL). The solution was acidified to pH = 5 by addition of 1 N HCl. The organic phase was separated, washed with water, saturated NaHCO<sub>3</sub>, and finally brine. The organic phase was dried over Na<sub>2</sub>SO<sub>4</sub>, filtered, and concentrated under reduced pressure to give **52** (2.0 g, 81%). This material was suitable for further use without purification (90% pure by analytical HPLC).

**3-Ethynyl-2-(2-methoxyethoxymethoxy)biphenyl (53).** The crude 2-(2-methoxyethoxymethoxy)biphenyl-3-carbaldehyde **52** (2 g, 6.7 mmol) was dissolved in dry MeOH (25 mL) and treated with K<sub>2</sub>CO<sub>3</sub> (2.9 g, 21 mmol). The (1-diazo-2-oxopropyl)phosphoric acid dimethyl ester<sup>25</sup> (2.7 g, 14.1 mmol) in MeOH (8 mL) was added dropwise over 5 min. The mixture was stirred overnight and then diluted with EtOAc. The mixture was washed with saturated NaHCO<sub>3</sub> solution. The organic phase was then washed with brine, dried over Na<sub>2</sub>SO<sub>4</sub>, filtered, and concentrated under reduced pressure. The residue was subjected to chromatography over silica gel eluting with 15% EtOAc in hexanes to give **53** (1.6 g, 66% from **10**). <sup>1</sup>H NMR (CDCl<sub>3</sub>) δ 7.52–7.31 (m, 7H), 7.13 (t, *J* = 7.4 Hz, 1H), 4.99 (s, 2H), 3.37–3.34 (m, 2H), 3.26 (s, 1H), 3.24 (s, 3H), 3.20–3.17 (m, 2H).

**2-[2-(2-Methoxyethoxymethoxy)biphenyl-3-yl]benzofuran-5-carbonitrile (54).** The 3-ethynyl-2-(2-methoxyethoxymethoxy)biphenyl **53** (1.6 g, 5.7 mmol) was mixed with 4-hydroxy-3-iodobenzonitrile **51** (1.4 g, 5.7 mmol) in dry DMF (50 mL). The mixture was then treated with dichlorobis(triphenylphosphine)palladium(II) (0.4 g, 0.57 mmol) followed by Et<sub>3</sub>N (4 mL, 28.7 mmol). The mixture was stirred for 30 min, and then CuI (0.22 g, 1.1 mmol) was added. The resultant mixture was stirred for 3 h and then diluted with EtOAc (150 mL). The organic solution was washed with brine, dried over Na<sub>2</sub>SO<sub>4</sub>, filtered, and concentrated under reduced pressure. The residue was subjected to chromatography over silica gel eluting with 20% EtOAc in hexanes to give **54** (0.53 g, 23%). <sup>1</sup>H NMR (CDCl<sub>3</sub>) δ 7.97 (dd, *J* = 8.3, 2.2 Hz, 1H), 7.94 (dd, *J* = 1.7, 0.8 Hz, 1H), 7.59–7.57 (m, 2H), 7.56 (dd, *J* = 3.3, 1.9 Hz, 1H), 7.52 (d, *J* = 0.8 Hz, 1H), 7.47–7.36 (m, 5H), 7.31 (t, *J* = 8.5 Hz, 1H), 4.72 (s, 2H), 3.29–3.25 (m, 2H), 3.21 (s, 3H), 3.20–3.15 (m, 2H).

**2-(2-Hydroxybiphenyl-3-yl)benzofuran-5-carboxamide (58).** The 2-[2-(2-methoxyethoxymethoxy)biphenyl-3-yl]benzofuran-5-carbonitrile **54** (0.53 g, 1.3 mmol) was dissolved in absolute EtOH (75 mL), and excess 50% aqueous hydroxylamine (2 mL) was added. The solution was refluxed for 2.5 h and then concentrated under reduced pressure to give **55**. The residue **55** was dissolved in THF (75 mL) and treated with acetic anhydride (0.25 mL, 2.7 mmol). The mixture was stirred for 30 min to form **56**, and then MeOH (25 mL) was added followed by 10% Pd/C (50 mg) catalyst. The mixture was stirred under hydrogen for 12 h and then filtered through Celite. The filtrate was concentrated under reduced pressure to give **57**. The crude residue **57** was dissolved in MeOH (75 mL) and treated with 6 N HCl (5 mL). The resultant mixture was stirred for 2 h and then concentrated under reduced pressure. The crude residue was subjected to preparative HPLC chromatography to give **58** (186 mg, 43%) as an amorphous white solid. <sup>1</sup>H NMR (DMSO-*d*<sub>6</sub>) δ 9.54 (br s, 2H), 9.36 (br m, 3H), 8.29 (s, 1H), 7.92–7.80 (m, 3H), 7.59–7.36 (m, 6H), 7.29 (dd, *J* = 7.4, 1.5 Hz, 1H), 7.13 (t, *J* = 8.6 Hz, 1H). <sup>13</sup>C NMR (DMSO-*d*<sub>6</sub>) δ 166.6, 156.5, 155.4, 151.9, 138.4, 132.3, 132.2, 130.1, 129.9, 129.1, 127.9, 126.7, 125.0, 123.5, 122.6, 121.5, 119.7, 112.0, 106.4. MS-Sciex *m/z* 328.6 [MH<sup>+</sup>]. Anal. (C<sub>21</sub>H<sub>16</sub>N<sub>2</sub>O<sub>2</sub>·HCl) C, H, N, O.

**Enzymology.** Enzymes were purchased as indicated: high molecular weight (HMW) u-PA (American Diagnostica), t-PA (Sigma), trypsin (Worthington), thrombin (Calbiochem), plasmin (Enzyme Research Labs), and factor Xa (Haematological Technologies, Inc.). The substrates for trypsin, plasmin, and

thrombin (tosyl-Gly-Pro-Lys-*p*-nitroanilide), and for factor Xa (CH<sub>3</sub>OCO-D-CHA-Gly-Arg-*p*NA-AcOH, "Pefachrome Xa") were from Centerchem, Inc. The substrate for HMW u-PA (Glt-Gly-Arg-AMC) was from Peptide Institute, and the substrate for t-PA (CH<sub>3</sub>-SO<sub>2</sub>-D-HHT-Gly-Arg-*p*NA, "Spectrozyme tPA") was from American Diagnostica.

**Enzyme Assays.** u-PA was assayed spectrofluorometrically, and all other enzymes were assayed spectrophotometrically. All enzymes were assayed at ambient temperature in 50 mM Tris, 150 mM NaCl, 0.05% (v/v) Tween-20, 10% (v/v) DMSO, 0.002% antifoam, pH = 7.4 with EDTA (1 mM). The thrombin and factor Xa assays also contained 5.0 mM CaCl<sub>2</sub>. The final concentrations of u-PA, t-PA, trypsin, thrombin, plasmin and factor Xa in the respective assays were 4 (or 5), 11 (or 15), 15, 10, 6 and 4 nM. The substrate concentrations of 85 μM (u-PA), 300 μM (t-PA), 25 or 45 μM (trypsin), 300 μM (thrombin), 130 μM (plasmin), and 550 μM (factor Xa) were chosen based on the determined *K<sub>m</sub>* values of 85, 500, 45, 300, 100, and 600 μM, respectively. For u-PA activity, the rate of change in relative fluorescence units (RFU) emitted at 460 nm (excitation at 355 nm) was measured immediately after addition of enzyme. For all other enzymatic activities, the rate of change in absorbance at 405 nm was measured immediately after addition of enzyme. Apparent inhibition constants, *K<sub>i</sub>'* values, were calculated from the velocity data generated at the various inhibitor concentrations using the software package *BatchKi* (developed and provided by Dr. Petr Kuzmich, Biokin Ltd., Madison, WI) using methodology similar to that described for tight-binding inhibitors.<sup>27</sup> *BatchKi* applies nonlinear regression analysis to return nominal likelihood intervals at the 65% confidence, using the logic described by Bates and Watts.<sup>29</sup> The *K<sub>i</sub>'* values are accepted where the nominal likelihood intervals at 65% confidence vary within 0.5 to 1.5-fold from the *K<sub>i</sub>'* values. These values were converted to *K<sub>i</sub>* values by the formula, *K<sub>i</sub>* = *K<sub>i</sub>'*/(1 + *S*/*K<sub>m</sub>*).

**Crystallization and Preparation of Protease-Inhibitor Complexes.** Procedures and conditions for crystallization have been reported by Katz et al.<sup>14</sup>

**Acknowledgment.** The authors are grateful to Dr. T. Jenkins, R. Day, Dr. D. McGee, and Dr. V. Tai for the synthesis of screening leads and late stage compounds. The authors also thank Dr. Mike Venuti and Dr. Jochen Knolle for helpful discussions and insights.

**Supporting Information Available:** Affinity measurements of selected compounds toward the panel of enzymes in the presence of zinc ions. This material is available free of charge via the Internet at <http://pubs.acs.org>.

## References

- (1) Katz, B. A.; Clark, J. M.; Finer-Moore, J. S.; Jenkins, T. E.; Johnson, C. R.; Ross, M. J.; Luong, C.; Moore, W. R.; Stroud, R. M. Design of Potent Selective Zinc-mediated Serine Protease Inhibitors. *Nature* **1998**, *391*, 608–612.
- (2) (a) Powers, J. C.; Harper, J. W. Inhibitors of serine proteinases. In *Proteinase Inhibitors*; Barrett, A. J., Salvesen, G., Eds.; Elsevier: Amsterdam, 1986. (b) Andreasen, P. A.; Kjoller, L.; Christensen, L.; Duffy, M. J. The Urokinase-type Plasminogen Activator System in Cancer Metastasis: A Review. *Int. J. Cancer* **1997**, *72*, 1–22. (c) Jackson, C. M.; Nemerson, Y. Blood Coagulation. *Annu. Rev. Biochem.* **1980**, *49*, 765–811. (d) Leung, D.; Abbenante, G.; Fairlie, D. P. Protease Inhibitors: Current Status and Future Prospects. *J. Med. Chem.* **2000**, *43*, 305–341. (e) Henkin, J. Proteases and Metastasis. *Annu. Rep. Med. Chem.* **1993**, *28*, 151–160.
- (3) (a) Sanderson, P. E. J.; Naylor-Olsen, A. M. Thrombin Inhibitor Design. *Curr. Med. Chem.* **1998**, *5*, 289–304. (b) Vacca, J. P. Thrombosis and Coagulation. *Annu. Rep. Med. Chem.* **1998**, *33*, 81–90.
- (4) Ripka, W. C.; Vlasuk, G. P. Antithrombotics/Serine Proteases. *Annu. Rep. Med. Chem.* **1997**, *32*, 71–89.
- (5) Fevig, J. M.; Wexler, R. R. Anticoagulants: Thrombin and Factor Xa Inhibitors. *Annu. Rep. Med. Chem.* **1999**, *34*, 81–100.
- (6) Magill, C.; Katz, B. A.; Mackman, R. L. Emerging Therapeutic Targets in Oncology: Urokinase-type Plasminogen Activator System. *Emerging Ther. Targets* **1999**, *3*, 109–133.

- (7) Rice, K. D.; Tanaka, R. D.; Katz, B. A.; Numerof, R. P.; Moore, W. R. Inhibitors of Trypsin-like Proteinases. Selective Cell-Mediated Diseases. *Curr. Pharm. Des.* **1998**, *4*, 381–396.
- (8) Mehdi, S. Synthetic and Naturally Occurring Protease Inhibitors Containing an Electrophilic Carbonyl Group. *Bioorg. Chem.* **1993**, *21*, 249–259.
- (9) Wakselman, M.; Xie, J.; Mazaleyrat, J.-P. New Mechanism-Based Inactivators of Trypsin-like Proteinases. Selective Inactivation of Urokinase by Functionalized Cyclopeptides Incorporating a Sulfoniomethyl-Substituted *m*-Aminobenzoic Acid Residue. *J. Med. Chem.* **1993**, *36*, 1539–1547.
- (10) Tamura, S. Y.; Weinhouse, M. I.; Roberts, C. A.; Goldman, E. A.; Masukawa, K.; Anderson, S. M.; Cohen, C. R.; Bradbury, A. E.; Bernardino, V. T.; Dixon, S. A.; Ma, M. G.; Nolan, T. G.; Brunck, T. K. Synthesis and Biological Activity of Peptidyl Aldehyde Urokinase Inhibitors. *Bioorg. Med. Chem. Lett.* **2000**, *10*, 983–987.
- (11) Deadman, J. J.; Elgendy, S.; Goodwin, C. A.; Green, D.; Baban, J. A.; Patel, G.; Skordalakes, E.; Chino, N.; Claeson, G.; Kakkar, V. V.; Scully, M. F. Characterization of a Class of Peptide Boronates with Neutral P1 Side Chains as Highly Selective Inhibitors of Thrombin. *J. Med. Chem.* **1995**, *38*, 1511–1522.
- (12) (a) Janc, J. W.; Clark, J. M.; Warne, R. L.; Elrod, K. C.; Katz, B. A.; Moore, W. R. A Novel Approach to Serine Protease Inhibition: Kinetic Characterization of Inhibitors Whose Potencies and Selectivities Are Dramatically Enhanced by Zinc(II). *Biochemistry*, **2000**, *39*, 4792–4800. (b) Axys Pharmaceuticals Inc. Bi-Amidino Group Substituted Heterocycle Derivatives and their use as Anticoagulants. Intl. Pat. Appl. 9926932, June 3, 1999. (c) Axys Pharmaceuticals Inc. Substituted Amidinoaryl Derivatives and their use as Anticoagulants. Intl. Pat. Appl. 9926933, June 3, 1999. (d) Axys Pharmaceuticals Inc. Substituted Amidinoaryl Derivatives and their use as Anticoagulants. Intl. Pat. Appl. 9926941, June 3, 1999.
- (13) Presnell, S. R.; Patil, G. S.; Mura, C.; Jude, K. M.; Conley, J. M.; Bertrand, J. A.; Kam, C.-M.; Powers, J. C.; Williams, L. D. Oxyanion-Mediated Inhibition of Serine Proteases. *Biochemistry* **1998**, *37*, 17068–17081.
- (14) Katz, B. A.; Elrod, K.; Luong, C.; Rice, M.; Mackman, R. L.; Sprengeler, P. A.; Spencer, J.; Hataye, J.; Janc, J.; Link, J.; Litvak, J.; Rai, R.; Rice, K.; Sideris, S.; Verner, E.; Young, W. A Novel Serine Protease Inhibition Motif Involving a Multi-centered Short Hydrogen Bonding Network at the Active Site. *J. Mol. Biol.* **2001**, *307*, 1451–1486.
- (15) Rai, R.; Kolesnikov, A.; Li, Y.; Young, W.; Leahy, E.; Sprengeler, P.; Verner, E.; Shrader, W.; Burgess-Henry, J.; Sangalang, J.; Allen, D.; Chen, X.; Katz, B.; Luong, C.; Elrod, K.; Cregar, L. Development of Potent and Selective Factor Xa Inhibitors. *Bioorg. Med. Chem. Lett.* In press.
- (16) Tidwell, R. R.; Geratz, J. D.; Dann, O.; Volz, G.; Zeh, D.; Loewe, H. Diarylamidine Derivatives with One or Both of the Aryl Moieties Consisting of an Indole or Indole-like Ring. Inhibitors of Arginine-Specific Esteroproteases. *J. Med. Chem.* **1978**, *21*, 613–623.
- (17) Fairley, T. A.; Tidwell, R. R.; Donkor, I.; Naiman, N. A.; Ohemeng, K. A.; Lombardy, R. J.; Bentley, J. A.; Cory, M. Structure, DNA Minor Groove Binding, and Base Pair Specificity of Alkyl- and Aryl-Linked Bis(amidinobenzimidazoles) and Bis(amidinoindoles). *J. Med. Chem.* **1993**, *36*, 1746–1753.
- (18) Geratz, J. D.; Stevens, F. M.; Polakoski, K. L.; Parrish, R. F.; Tidwell, R. R. Amidino-Substituted Aromatic Heterocycles as Probes of the Specificity Pocket of Trypsin-Like Proteases. *Arch. Biochem. Biophys.* **1979**, *197*, 551–559.
- (19) (a) Lombardy, R. L.; Tanious, F. A.; Ramachandran, K.; Tidwell, R. R.; Wilson, W. D. Synthesis and DNA Interactions of Benzimidazole Dications Which Have Activity against Opportunistic Infections. *J. Med. Chem.* **1996**, *39*, 1452–1462. (b) Singh, M. P.; Sasmal, S.; Lu, W.; Chatterjee, M. N. Synthetic Utility of Catalytic Fe(III)/Fe(II) Redox Cycling Towards Fused Heterocycles: A Facile Access to Substituted Benzimidazole, Bis-benzimidazole and Imidazopyridine Derivatives. *Synthesis* **2000**, *10*, 1380–1390.
- (20) Hofsløkken, N. U.; Skattebøl, L. Convenient Method for the *ortho*-Formylation of Phenols. *Acta Chem. Scand.* **1999**, *53*, 258–262.
- (21) Iwanowicz, E. J.; Lau, W. F.; Lin, J.; Roberts, D. G. M.; Seiler, S. M. Derivatives of 5-Amidine Indole as Inhibitors of Thrombin Catalytic Activity. *Bioorg. Med. Chem. Lett.* **1996**, *6*, 1339–1344.
- (22) Robinson, B. *The Fischer Indole Synthesis*; John Wiley and Sons: New York, 1982.
- (23) Castro, J. L.; Baker, R.; Guiblin, A. R.; Hobbs, S. C.; Jenkins, M. R.; Russell, M. G. N.; Beer, M. S.; Stanton, J. A.; Scholey, K.; Hargreaves, R. J.; Graham, M. I.; Matassa, V. G. Synthesis and Biological Activity of 3-[2-(Dimethylamino)ethyl]-5-[(1,1-dioxo-5-methyl-1,2,5-thiadiazolidin-2-yl)-methyl]-1*H*-indole and Analogues: Agonists for the 5-HT<sub>1D</sub> Receptor. *J. Med. Chem.* **1994**, *37*, 3023–3032.
- (24) Miyaoura, N.; Yanagi, T.; Suzuki, A. The Palladium-catalyzed Cross-coupling Reaction of Phenylboronic Acid with Haloarenes in the Presence of Bases. *Synth. Commun.* **1981**, *11*, 513–519.
- (25) Müller, S.; Liepold, B.; Roth, G. J.; Bestmann, H. J. An Improved One-pot Procedure for the Synthesis of Alkynes from Aldehydes. *Synlett* **1996**, *6*, 521–522.
- (26) Candiani, I.; DeBernardinis, S.; Cabri, W.; Marchi, M.; Bedeschi, A.; Penco, S. A Facile One-pot Synthesis of Polyfunctionalized 2-Unsubstituted Benzo[b]furans. *Synlett* **1993**, *4*, 269–270.
- (27) Kuzmic, P.; Sideris, S.; Cregar, L. M.; Elrod, K. C.; Rice, K. D.; Janc, J. W. High-Throughput Screening of Enzyme Inhibitors: Automatic Determination of Tight-Binding Inhibition Constants. *Anal. Biochem.* **2000**, *281*, 62–67.
- (28) (a) Katz, B. A.; Mackman, R.; Luong, C.; Radika, K.; Martelli, A.; Sprengeler, P. A.; Wang, J.; Chan, H.; Wong, L. Structural Basis for Selectivity of a Small Molecule S1-binding Submicromolar Inhibitor of Urokinase-type Plasminogen Activator. *Chem. Biol.* **2000**, *7*, 299–312. (b) Nienaber, V.; Wang, J.; Davidson, D.; Henkin, J. Re-engineering of Human Urokinase Provides a System for Structure-based Drug Design at High Resolution and Reveals a Novel Structural Subsite. *J. Biol. Chem.* **2000**, *275*, 7239–7248. (c) Nienaber, V. L.; Davidson, D.; Edalji, R.; Giranda, V. L.; Klinghofer, V.; Henkin, J.; Magdalinos, P.; Mantei, R.; Merrick, S.; Severin, J. M.; Smith, R. A.; Stewart, K.; Walter, K.; Wang, J.; Wendt, M.; Weitzberg, M.; Zhao, X.; Rockway, T. Structure-directed Discovery of Potent Non-peptidic Inhibitors of Human Urokinase that Access a Novel Binding Subsite. *Structure* **2000**, *8*, 553–563. (d) Sperl, S.; Jacob, U.; Arroyo de Prada, N.; Stürzebecher, J.; Wilhelm, O. G.; Bode, W.; Magdolen, V.; Huber, R.; Moroder, L. (4-Aminomethyl)phenylguanidine Derivatives as Nonpeptidic Highly Selective Inhibitors of Human Urokinase. *Proc. Natl. Acad. Sci. U.S.A.* **2000**, *97*, 5113–5118. (e) Zeslawski, E.; Schweinitz, A.; Karcher, A.; Sonnermann, P.; Sperl, S.; Stürzebecher, J.; Jacob, U. Crystals of the Urokinase Type Plasminogen Activator Variant  $\beta$ c-uPA in Complex with Small Molecule Inhibitors Opens the Way towards Structure-based Drug Design. *J. Mol. Biol.* **2000**, *301*, 465–475.
- (29) Bates, D. M.; Watts, D. W. *Nonlinear Regression and its Applications*. John Wiley and Sons: New York, 1988.

JM0100638